https://doi.org/10.5194/egusphere-2026-3055
Preprint. Discussion started: 26 June 2026

Taxon-specific coccolithophore carbonate stocks and production across a Pacific trophic gradient from oligotrophic gyre to upwelling zone

Guillaume Lassus[1,2], Luc Beaufort[1], Martine Couapel[1*], David Mendels[2]

[1]Aix-Marseille Université, CNRS, IRD, INRAE, CEREGE, Aix-en-Provence, France
[2]ZORTH, 10, Rue Mazarine, 13100, Aix-en-Provence, France
[*]Present address: MARBEC, Avenue Jean Monnet, Sète, France

Correspondence to: Guillaume Lassus (guillaume.lassus8@orange.fr)

Abstract. Coccolithophores contribute substantially to marine carbonate production, yet species-resolved estimates of coccosphere-associated $CaCO_3$ stocks remain scarce across large-scale trophic gradients. Here we quantify multispecific coccosphere carbonate inventories and first-order production estimates along the BIOSOPE transect across the South Pacific Gyre, one of the most strongly stratified regions of the global ocean. Estimates were obtained using an upgraded SYRACO automated recognition workflow combined with bidirectional circular polarization (BCP) imaging, allowing direct reconstruction of coccosphere calcite content at the cellular scale. Coccolithophore assemblages reproduced the major regional and vertical ecological structures previously described across the transect, including the transition from nutrient-rich surface communities near the Marquesas Archipelago and the eastern upwelling-influenced region to vertically structured assemblages in the oligotrophic gyre. At the transect scale, $CaCO_3$ standing stocks were primarily controlled by these large-scale trophic gradients, with maxima located in surface waters of mesotrophic regions and at depth within the deep chlorophyll maximum in the stratified gyre, indicating a vertical decoupling between coccosphere abundance and carbonate inventories under oligotrophic conditions. Taxon-specific analyses show that carbonate inventories reflect both coccosphere abundance and strong interspecific contrasts in calcite content. Isochrysidales, particularly *Emiliania huxleyi*, dominated carbonate stocks through their numerical abundance, whereas more heavily calcified taxa contributed disproportionately relative to their cell densities. Despite structuring assemblages in the lower euphotic zone, deep-dwelling taxa represented only a minor fraction of suspended carbonate stocks in the water column, contrasting with their major contribution to sedimentary assemblages in oligotrophic regions. First-order $CaCO_3$ production estimates followed spatial patterns similar to standing stocks, with enhanced production in mesotrophic regions and a sustained contribution from oligotrophic communities. Although uncertainties remain related to species-specific growth rates, these estimates provide the first multispecific constraints on coccolithophore calcification dynamics in the southeastern Pacific. Overall, this study demonstrates that combining automated coccosphere recognition with BCP-based carbonate measurements provides a robust framework for resolving species-level carbonate inventories across major oceanic trophic gradients and represents an important step toward quantitative assessments of coccolithophore contributions to pelagic carbonate cycling at basin scale.

https://doi.org/10.5194/egusphere-2026-3055
Preprint. Discussion started: 26 June 2026

1 Introduction

Calcifying planktonic organisms play a central role in the marine carbon cycle. The calcium carbonate ($CaCO_3$) they produce strongly affects marine carbon chemistry and, indirectly, atmospheric CO_2 (Broecker and Peng, 1982; Archer, 1996; Sarmiento and Gruber, 2006). Through their sedimentation, these organisms directly contribute to the export of carbonates to the deep ocean (Sundquist and Broecker, 1985; Milliman, 1993; Millero, 2007; Ziveri et al., 2007). Most pelagic marine $CaCO_3$ is produced by coccolithophores and foraminifera as calcite (Neukermans et al., 2023; Ziveri et al., 2023), and by planktonic gastropods as aragonite (Buitenhuis et al., 2019; Sulpis et al., 2022; Knecht et al., 2023). Quantifying the respective contributions of these groups is therefore essential to estimate carbonate production and, ultimately, carbonate sequestration in marine sediments (Neukermans et al., 2023; Ziveri et al., 2023; Kruijt et al., 2025).

Coccolithophores are ubiquitous components of marine phytoplankton communities and generally account for 10–20 % of global phytoplankton primary production (Poulton et al., 2007). Within the euphotic zone, they represent a dominant fraction of pelagic $CaCO_3$ production, contributing on average 68–79 % of the total $CaCO_3$ inventory in the North Pacific Ocean (Ziveri et al., 2023; Han et al., 2025) and approximately 80 % in the South Atlantic Ocean (Kruijt et al., 2025). Despite this major contribution, the respective roles of individual coccolithophore taxa in structuring carbonate standing stocks remain insufficiently constrained, particularly in oligotrophic regions of the open ocean where communities are vertically stratified and taxonomically diverse.

This limitation partly reflects the strong interspecific variability in coccosphere calcite mass. Calcification rates and coccosphere mass differ substantially among taxa (Beaufort and Heussner, 1999; Young and Ziveri, 2000; Daniels et al., 2014, 2016), implying that the most abundant species are not necessarily the dominant contributors to particulate $CaCO_3$ inventories. Reliable estimates of carbonate standing stocks therefore require taxon-resolved approaches combining abundance measurements with direct estimates of individual coccosphere calcite content.

Quantifying coccolithophore carbonate production remains methodologically challenging. Satellite-based approaches cannot resolve species composition or detect populations below the upper tens of meters of the water column (Brown and Yoder, 1994; Balch et al., 2007, 2018; Daniels et al., 2018). Optical estimates based on detached coccolith morphometry provide valuable constraints but do not fully capture variability at the coccosphere level, where both coccolith number and size may vary within populations and even within individual life cycles (Daniels et al., 2014; Beuvier et al., 2019; Suchéras-Marx et al., 2021). Direct multispecific estimates of coccosphere-associated carbonate standing stocks therefore remain scarce, especially in oligotrophic oceanic regions. Recent developments in bidirectional circular polarization microscopy now allow direct estimation of coccolith thickness and coccosphere calcite mass independently of microscope calibration (Beaufort et al., 2021), while advances in deep-learning-based recognition enable automated identification of coccospheres across multiple taxa. These methodological advances now make it possible to quantify taxon-specific contributions to coccosphere-associated carbonate inventories at the scale of entire oceanic transects.

The South-East Pacific Gyre represents one of the most oligotrophic regions of the global ocean but also one of the least constrained in terms of coccolithophore carbonate inventories (Claustre and Maritorena, 2003). Along the BIOSOPE transect, Beaufort et al. (2008) provided the first automated estimates of coccosphere-associated carbonate stocks for Isochrysidales, showing a strong vertical structuring of their distribution along the deep chlorophyll maximum. However, the contribution of other coccolithophore groups to carbonate standing stocks along this major trophic gradient remains largely unresolved.

https://doi.org/10.5194/egusphere-2026-3055
Preprint. Discussion started: 26 June 2026

Here, we combine these approaches within an upgraded SYRACO framework, including the development of a dedicated processing pipeline and systematic expert validation of automated identifications, to provide the first multispecific estimate of coccosphere-associated $CaCO_3$ standing stocks along the BIOSOPE transect and to quantify the taxon-specific contributions of coccolithophore communities across the trophic gradient of the South Pacific Gyre.

2 Materials and methods

2.1 Setting

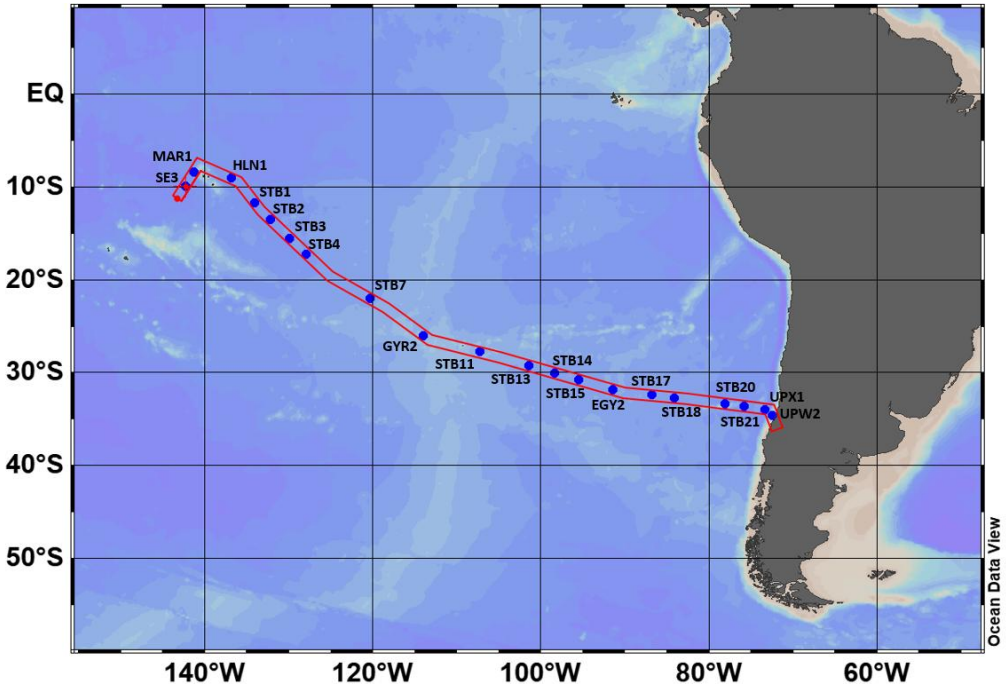

Figure 1 Map of the Southeastern Pacific Ocean showing sampling stations (blue dots) along the BIOSOPE transect (red outline).

During the BIOSOPE cruise, conducted in the South-East Pacific aboard the research vessel *Atalante* from October 26th to December 11th, 2004, an 8000 km transect was carried out. This sampling strategy covered a wide range of contrasted trophic environments (Fig. 1): In the western and eastern sectors, stations located near the Marquesas Archipelago (142–130° W) and in the transition zone (100–80° W) between the South Pacific Gyre (SPG) and the Peru–Chile Upwelling (PCU) are nutrient-rich systems (Claustre et al., 2008; Beaufort et al., 2008). The enrichment of waters around the Marquesas is partly linked to the influence of the South Equatorial Current (SEC), while the eastern region benefits from nutrient inputs associated with coastal upwelling. In these regions, maximum chlorophyll concentrations are observed at shallow depths, usually between 50 and 100 m (Claustre et al., 2008; Ras et al., 2008). In contrast, the central South Pacific Gyre (SPG, 130–100° W) is one of the most oligotrophic oceanic regions worldwide, characterized by one of the lowest surface chlorophyll concentrations, as well as a

https://doi.org/10.5194/egusphere-2026-3055
Preprint. Discussion started: 26 June 2026

particularly deep pycnocline (>200 m) (Claustre et al., 2008). This region also displays strong water column stratification, with a particularly stable deep chlorophyll maximum (DCM) occurring at depths between 160 and 200 m (Claustre et al., 2008; Cornec et al., 2021). This marked trophic gradient provides a suitable framework to investigate variations in coccolithophore abundance and community composition along the transect.

2.2 Coccolithophores

The composition of contemporary coccolithophore communities varies strongly with latitude and depth as a function of nutrient availability and light exposure (Okada and McIntyre, 1979; Winter and Siesser, 1994; Boeckel and Baumann, 2008; O'Brien et al., 2013; Poulton et al., 2017). In nutrient-rich and weakly stratified environments such as the Marquesas region and the Peru–Chile Upwelling transition zone, assemblages are typically dominated by Isochrysidales, particularly *Emiliania huxleyi* and *Gephyrocapsa* (Okada and Honjo, 1973; Beaufort and Heussner, 1999; Tyrrell and Merico, 2004; Baumann et al., 2008; Keuter et al., 2022; Guerreiro et al., 2023; Han et al., 2025). In contrast, the strongly stratified oligotrophic waters of the South Pacific Gyre generally host more diverse assemblages dominated by *Umbellosphaera* in the upper euphotic zone and *Florisphaera profunda* near the DCM, together with representatives of Syracosphaerales such as *Syracosphaera*, *Discosphaera* and *Rhabdosphaera*, and deeper-dwelling taxa including *Gladiolithus* and *Algirosphaera* (Okada and Honjo, 1973; Kinkel et al., 2000; Baumann et al., 2008; Dimiza et al., 2016; Poulton et al., 2017; Keuter et al., 2022; Guerreiro et al., 2023; Han et al., 2025). Because coccosphere calcite mass differs substantially among these taxa (Beaufort and Heussner, 1999; Young and Ziveri, 2000; Daniels et al., 2014, 2016), this ecological gradient provides a suitable framework for assessing their respective contributions to coccolithophore-associated $CaCO_3$ standing stocks along the BIOSOPE transect.

2.3 Sampling

Coccolithophore samples were collected at 20 stations, with sampling depths defined relative to the deep chlorophyll maximum, which is located near the pycnocline and is considered a major intra-oceanic ecotone (Longhurst, 1998). Water samples were collected at six characteristic depths: the first sample was taken at the surface (0–5 m), two samples were collected between 5 m and the depth of the DCM, followed by one sample within the DCM itself, and finally two additional samples were collected below the DCM. This sampling strategy allowed us to characterize coccolithophore communities on both sides of this key ecological boundary.

2.4 Sample processing

For most samples, approximately 4 L of seawater were filtered through a cellulose nitrate membrane with a diameter of 47 mm and a pore size of 0.45 µm. The membranes were then dried up and stored at room temperature. For the four stations located in the PCU region (stations STB20 to UPX2, 80–72° W), a filtration membrane with a diameter of 23 mm was used. In the laboratory, one quarter of each membrane was isolated and mounted between a microscope slide and coverslip, then sealed with Canada balsam to render the membrane transparent for optical analysis.

2.5 Image acquisition

https://doi.org/10.5194/egusphere-2026-3055
Preprint. Discussion started: 26 June 2026

For each BIOSOPE sample, a total of 300 adjacent contiguous fields were captured using a Hamamatsu ORCA camera (16-bit, 4 Mpixel, monochrome) mounted on an automated Leica polarizing microscope equipped with a ×100 oil-immersion objective, corresponding to a field area of 15 625 µm². Images were acquired using the universal bidirectional circular polarization method described by Beaufort et al. (2021), combined with monochromatic blue illumination (460 nm ± 10 nm, Chroma).

For each x–y position, twenty-four images were captured at twelve focal depths within a vertical range of approximately 10 µm, first under left circular polarization and then under right circular polarization. For each focal level, the images acquired under left and right circular polarization were first combined by calculating their intensity difference, producing a stack of thickness-sensitive images. These resulting stacks were subsequently combined using a multifocal reconstruction procedure to generate a single composite image containing the best-focused birefringent signal for each object in the field. The intensity of this signal is linearly proportional to calcite thickness, allowing direct estimation of coccolith and coccosphere calcite mass independently of microscope light calibration (Beaufort et al., 2021).

2.6 Image recognition

https://doi.org/10.5194/egusphere-2026-3055
Preprint. Discussion started: 26 June 2026

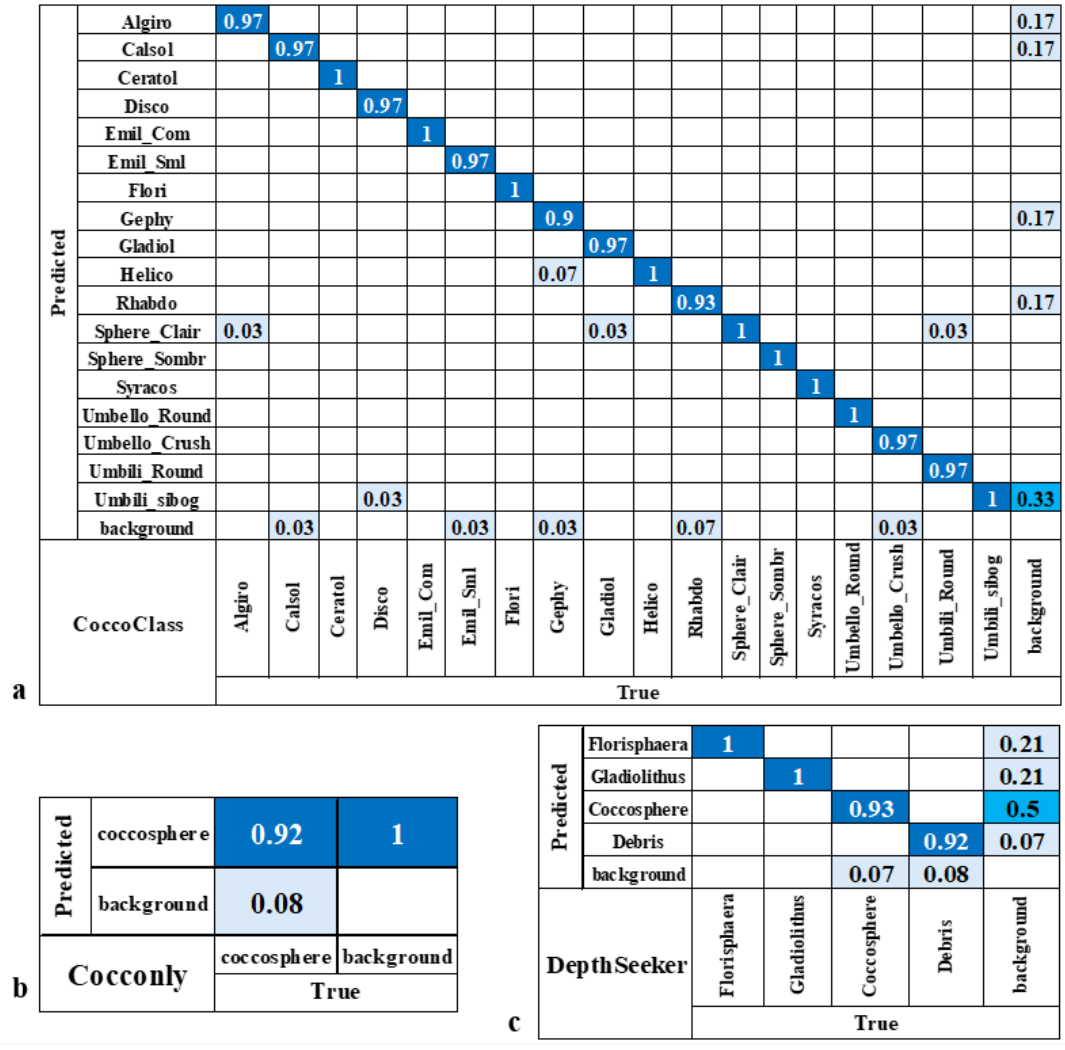

Figure 2 Reconstitution of normalized confusion matrixes for the **(a)** CoccoClass, **(b)** Cocconly, and **(c)** DepthSeeker recognition models. "Predicted" refers to expected results for a given class, while "True" indicates how many results match with predictions : 0 indicates that found objects count as false positives, whereas 1 indicates that found objects count as true positives. Blue hue shades highlight values (light blue: false positives, dark blue: true positives). Model classes abbreviations are: *Algirosphaera* (Algiro), *Calciosolenia* (Calsol), *Ceratolithus* (Ceratol), *Discosphaera* (Disco), *Emiliania huxleyi* (Emil_Com, Emil_Sml), *Florisphaera profunda* (Flori), *Gephyrocapsa* (Gephy), *Gladiolithus* (Gladiol), *Helicosphaera* (Helico), *Rhabdosphaera* (Rhabdo), Calcidiscaceae (Sphere_Clair, Sphere_sombr), Syracosphaeraceae (Syracos), *Umbellosphaera* (Umbello_Round, Umbello_Crush), *Umbilicosphaera* spp. (Umbili_Round), and *Umbilicosphaera sibogae* (Umbili_sibog).

Coccolithophore instances were automatically detected and measured using a modified version of the SYRACO software (Beaufort and Dollfus, 2004) integrating an object-detection module based on YOLOv8 (Jocher et al.,

https://doi.org/10.5194/egusphere-2026-3055
Preprint. Discussion started: 26 June 2026

2023). YOLO ("You Only Look Once") is a fast open-source algorithm specialized in object detection and classification (Redmon et al., 2016) that has previously been applied to the detection of morphologically variable microscopic objects such as blood cells (Alam and Islam, 2019).

The training dataset included 15 classes representing the main coccolithophore groups observed in BIOSOPE images, following the taxonomy of Young et al. (2003) and the Nannotax database (Young et al., 2022). Because YOLOv8 primarily relies on object shape recognition, classes were defined based on coccosphere morphology rather than strict taxonomic resolution in order to maximize detection robustness.

Isochrysidales were separated into two classes (*Emiliania* and *Gephyrocapsa*), while Syracosphaerales were divided into four classes (Syracosphaeraceae, *Calciosolenia*, *Discosphaera*, and *Rhabdosphaera*). Within Coccolithales, most *Umbilicosphaera* species were grouped into a single class (*Umbilicosphaera* spp.), whereas *U. sibogae* was treated separately because of its larger coccosphere size. Genera *Calcidiscus* and *Oolithotus* were grouped into a single class (Calcidiscaceae) to improve discrimination from *Umbilicosphaera*. Deep-photic-zone taxa included *Florisphaera*, *Gladiolithus*, and *Algirosphaera*. Additional detected classes included *Umbellosphaera*, *Helicosphaera*, and *Ceratolithus*.

Training annotations were produced manually by an expert user using bounding boxes defining individual coccospheres on bidirectional circular polarization images from samples collected during the independent CARACALHIS cruise in the Caribbean (Ellouz-Zimmermann and Beaufort, 2015), in order to avoid training bias from BIOSOPE material. Annotated classes were assigned based on coccosphere morphology following the taxonomy of Young et al. (2003) and the Nannotax database (Young et al., 2022).

Models were trained using images acquired under bidirectional circular polarization. Because SYRACO performance strongly depends on the number of training instances per class, with several thousand images generally required for robust detection, some taxa remained underrepresented. Dominant genera such as *Emiliania* and *Gephyrocapsa* were represented by more than 1,000 training instances, whereas fewer than 200 individuals were available for rarer taxa such as *Discosphaera*, *Rhabdosphaera*, *Florisphaera profunda*, and *Gladiolithus*. To improve model performance, these underrepresented classes were expanded using data augmentation procedures including rotation and image-quality transformations.

A hierarchical object-detection workflow was implemented to improve coccosphere recognition. First, coccospheres were detected as a single morphological class using the model "Cocconly", allowing the extraction of candidate coccosphere images independently of their taxonomic identity. This initial detection step ensured robust identification of birefringent coccospheres prior to taxonomic classification.

Extracted coccosphere images were subsequently assigned to taxonomic groups using a classification model, "Coccoclass", trained on coccosphere morphology. This two-step approach allowed separation between object detection and taxonomic attribution, thereby reducing false positives associated with direct multispecies detection. Preliminary results nevertheless showed confusion and limited detection of the deep-dwelling taxa *Florisphaera* and *Gladiolithus*. Because these taxa are critical for estimating carbonate standing stocks at depth, a third model ("DepthSeeker") was specifically developed to improve their recognition. This model included three classes: *Florisphaera*, *Gladiolithus*, and a generic "coccospheres" class grouping all remaining taxa. *Florisphaera* and *Gladiolithus* abundances used in this study were therefore derived from DepthSeeker outputs, whereas all remaining coccolithophore taxa were quantified using the Cocconly - Coccoclass classification workflow.

https://doi.org/10.5194/egusphere-2026-3055
Preprint. Discussion started: 26 June 2026

Confusion matrices illustrating model performance are provided in Fig. 2a–c and demonstrate that this hierarchical detection strategy allowed robust identification of morphologically distinct coccospheres while minimizing misclassification of deep-dwelling taxa that are known to be difficult to discriminate under automated recognition.

This workflow was applied to all BIOSOPE samples except the following. Sample MAR1_3 was damaged and could not be captured. The content of sample EGY_3 was not visible to SYRACO due to its opacity. In addition, frequent losses of focus occurred in sparsely populated samples, leading to image blurring and reduced visibility of birefringent particles, which complicated taxonomic recognition. As a result, all samples collected below 230 m (STB7_1, STB11_1, STB11_2, and STB14_1), together with samples STB14_4 and STB17_1, were considered non-representative and excluded from the analyses. Furthermore, at the PCU stations (STB20, STB21, UPX1, and UPW2), filtration was performed using smaller filters (25 mm diameter instead of 47 mm for the rest of the transect) because of the higher particle concentrations encountered in these productive waters. Although 4 L of seawater were nominally filtered at each station, filtration had to be forced due to rapid filter clogging, resulting in uncertainty in the effective filtered volume. Because this prevented reliable estimation of coccolithophore concentrations and associated $CaCO_3$ standing stocks, these stations were excluded from further analyses. The study therefore focuses on the remainder of the transect (142–80° W).

2.7 Data processing

For each taxon analyzed, the number of coccospheres per sample was determined using both SYRACO automatic detection and manual counting by an expert user. Coccosphere diameters (µm) and masses (pg) were determined using SYRACO only.

Maps and section plots were produced using Ocean Data View (ODV; Schlitzer, 2026).

2.7.1 Relative and absolute abundances

Based on the number of individuals, total and taxon-specific concentrations (cells mL^{-1}) were calculated for each sample using Eq. (1):

$$\text{Concentration} = \frac{NS}{PFV} \quad (1)$$

where N is the number of individuals counted, P is the number of fields captured per sample, S is the filter surface area (mm^2), F is the field surface area (mm^2), and V is the volume of seawater filtered per sample (mL). Absolute taxon abundances were vertically integrated by station and along the entire transect using the trapezoidal rule. Species assemblages were determined from relative abundances within the water column between 0 and 230 m depth, corresponding to the regional and transect-wide average maximal sampling depth. To assess the reliability of SYRACO-derived estimates, taxon-specific concentrations were compared with manual counts performed independently by an expert user on a separate dataset of 300 fields per sample using a linearly polarized light microscope with a field area of 31,416 μm^2. A correction factor of 2.01 was applied to account for differences in field surface area between both approaches. Correlations between SYRACO and manual counts were quantified using Pearson correlation coefficients (n = 80 samples). A principal component analysis (PCA) was also performed to examine the distribution of taxa among samples.

2.7.2 Average diameter

https://doi.org/10.5194/egusphere-2026-3055
Preprint. Discussion started: 26 June 2026

Most coccospheres exhibited a spherical or ovoid morphology. However, many instances were incomplete, having lost part of their coccoliths, and some taxa, such as *Calciosolenia*, displayed an elongated morphology, making diameter measurements less straightforward. Therefore, we used the maximum Feret diameter to provide a representative estimate of coccosphere size.

2.7.3 Average mass

Coccosphere calcite mass was estimated using bidirectional circular polarization (BCP) microscopy, which allows direct quantification of calcite thickness from birefringence phase differences (Beaufort et al., 2022). Thickness measurements obtained with this method are more precise than estimates based on coccolith length and width because they rely on optical phase retardation measurements with nanometer-scale sensitivity rather than geometric approximations. Calcite thickness was converted into mass using the density of calcite (2.71 g cm^{-3}).

BCP-derived coccosphere calcite mass estimates have been independently validated through comparison with volumetric measurements obtained using X-ray nanotomography on coccospheres of several Isochrysidales species (Beuvier et al., 2019), demonstrating the reliability of this approach for taxa whose crystallographic c-axis is oriented perpendicular to the optical trajectory.

However, in some coccolithophore groups such as Coccolithales and Zygodiscales, parts of the coccolith structure include calcite elements oriented parallel to the optical trajectory (Young et al., 2003). These elements do not contribute to birefringence signals and therefore remain undetected in BCP images, leading to systematic underestimation of coccosphere calcite mass if uncorrected. For example, in Coccolithales, only the proximal shield and the collar contribute to the birefringence signal. To account for this limitation, correction factors were applied based on structural reconstructions of coccolith architecture (Young et al., 2003, 2022) and on the correction approach proposed by Cubillos et al. (2012) for *Coccolithus pelagicus*. Correction factors of 1.4 for *Helicosphaera* and *Syracosphaera* spp, 1.6 for *Umbilicosphaera* spp. and *U. sibogae*, and 2.2 for Calcidiscaceae were applied to average coccosphere mass estimates. These corrected values provide improved first-order estimates of coccosphere calcite mass and therefore of their contribution to carbonate standing stocks.

For taxa represented by fewer than 10 individuals in a sample, sample-specific morphometric estimates were replaced by the average coccosphere mass calculated from the entire BIOSOPE transect for that taxon. This average value was then multiplied by coccosphere abundance to estimate carbonate standing stocks.

2.7.4 $CaCO_3$ stock distribution and taxa contributions

Because intact coccospheres mainly represent recently produced calcite associated with the contemporary coccolithophore population, whereas free coccoliths may include a substantial contribution from previously detached elements transported within the water column, coccosphere abundance and individual mass were used to estimate coccolithophore-associated $CaCO_3$ standing stocks (pg mL^{-1}) using Eq. (2):

$$CaCO_3 \text{ Quantity} = \frac{MNS}{PFV} \quad (2)$$

where M is the average individual coccosphere mass per sample, N is the number of individuals, P is the number of fields captured per sample, S is the filter surface area (mm^2), F is the field surface area (mm^2), and V is the volume of seawater filtered per sample (mL). The resulting $CaCO_3$ stock values were then used to determine carbonate distribution, along with the global and localized relative contribution of each taxon.

https://doi.org/10.5194/egusphere-2026-3055
Preprint. Discussion started: 26 June 2026

The resulting absolute $CaCO_3$ stock values were vertically integrated at each station and subsequently integrated along the transect using the trapezoidal rule. Similarly to abundances, overall and localized taxa contributions were represented based on relative $CaCO_3$ stocks and on regional and transect-wide mean maximal sampling depth.

2.7.5 $CaCO_3$ production rates estimates

After describing the spatial and taxonomic distribution of $CaCO_3$ standing stocks, we estimated first-order $CaCO_3$ production rates in order to evaluate the potential contribution of coccolithophores to calcite production along the transect. Because in situ growth rates were not available for the sampled communities, production rates were estimated using published laboratory maximum specific growth rates (μmax), providing upper-bound approximations of potential calcite production. Production rates were calculated using Eq. (3):

$$\text{Production rate} = CW\mu \quad (3)$$

where C is the vertically integrated coccosphere concentration (cells m^{-2}), W is the taxon-specific average coccosphere mass at the transect scale (μg $CaCO_3$ $cell^{-1}$), and μ is the taxon-specific growth rate (d^{-1}).

Maximum specific growth rates (μmax) were taken from published laboratory estimates for *Emiliania huxleyi*, *Gephyrocapsa*, *Syracosphaera pulchra*, *Calcidiscus leptoporus*, and *Helicosphaera carteri* (Sett et al., 2014; Fiorini et al., 2011; Diner et al., 2015; Bianco et al., 2025b; Ziveri et al., 2025). Growth rates of *S. pulchra* were applied to all Syracosphaerales, while those of *C. leptoporus* were applied to Calcidiscaceae. Production rates for *Umbellosphaera*, *Ceratolithus*, *Algirosphaera*, *Florisphaera profunda*, and *Gladiolithus* were estimated using the minimum growth rate reported for *C. leptoporus* (Diner et al., 2015).

Because coccolithophore growth rates strongly depend on environmental conditions such as light availability, temperature, and nutrient concentrations, which vary markedly along the BIOSOPE transect, these estimates should be considered first-order approximations of potential production rather than direct measurements of in situ calcification rates.

3 Results

3.1 Coccolithophores Abundances

3.1.1 Spatial distribution

https://doi.org/10.5194/egusphere-2026-3055
Preprint. Discussion started: 26 June 2026

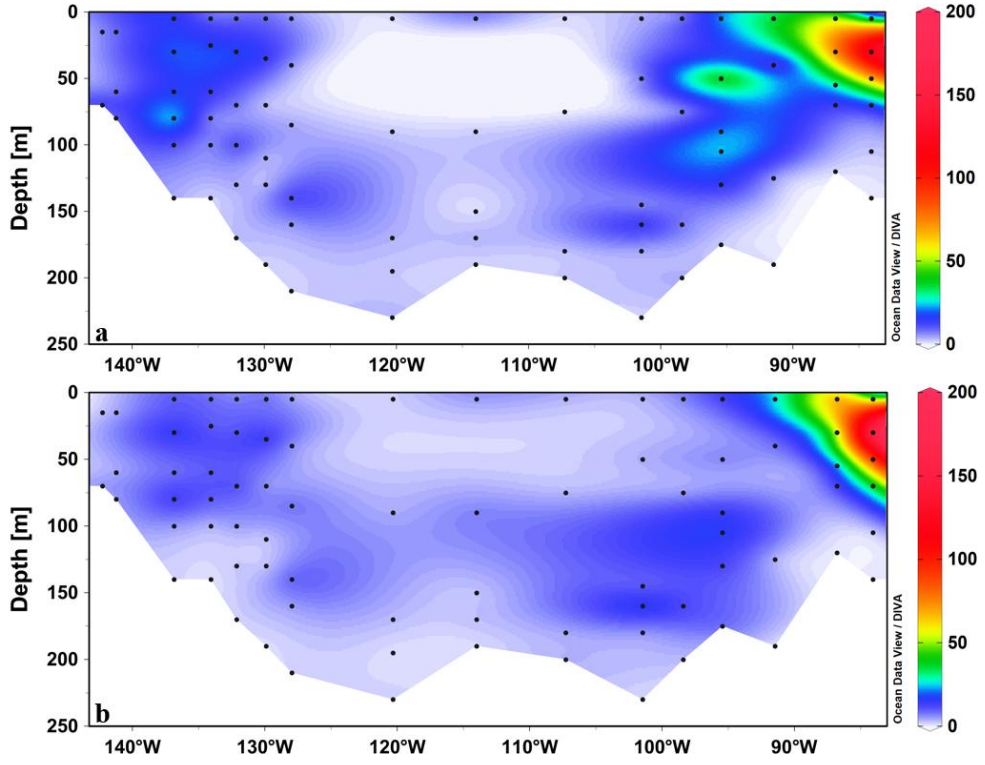

Figure 3 Vertical distribution of Coccolithophores abundance (coccosphere ml^{-1}) vertical distribution along sampled depth (black dots) of the BIOSOPE transect obtained from **(a)** SYRACO and **(b)** manual-based counts.

When vertically integrated across depths and along the transect (142–80° W), total coccosphere standing stocks reached 8.58 × 10^{15} cells m^{-1} in SYRACO and 8.04 × 10^{15} cells m^{-1} in manual counts. Mean concentrations were similar between both datasets, averaging 7.58 cells mL^{-1} (SYRACO) and 7.10 cells mL^{-1} (manual counts), with nearly identical median values (5.74 and 5.75 cells mL^{-1}, respectively). Coccosphere concentrations ranged from 0.96 to 36.53 cells mL^{-1} in SYRACO counts and from 2.67 to 51.62 cells mL^{-1} in manual counts. In both datasets, coccolithophore abundances were generally higher in nutrient-rich regions, with maximum concentrations observed at the easternmost sampling station (Fig. 3a and b).

At the transect scale, coccolithophore assemblages were dominated by Isochrysidales together with the genus *Umbellosphaera*. Mean concentrations of *Emiliania huxleyi*, *Gephyrocapsa*, and *Umbellosphaera* reached 3.59, 0.99, and 1.05 cells mL^{-1} in SYRACO counts, compared with 3.29, 1.33, and 1.13 cells mL^{-1} in manual counts. *Emiliania huxleyi* was especially abundant in the upper euphotic zone (0–100 m) of the eastern region, whereas *Gephyrocapsa* was more prevalent near the Marquesas in the western sector.

Within the Syracosphaerales, Syracosphaeraceae represented the dominant group in SYRACO counts (0.42 cells mL^{-1} on average), whereas manual counts indicated higher abundances of *Rhabdosphaera* (0.29 cells mL^{-1}). Syracosphaeraceae coccospheres were distributed throughout the upper 200 m of the water column and were more abundant in the eastern region. In manual counts, their concentrations averaged 0.17 cells mL^{-1}, with a slight increase between 50 and 100 m near the Marquesas. *Discosphaera* and *Rhabdosphaera* displayed similar

https://doi.org/10.5194/egusphere-2026-3055
Preprint. Discussion started: 26 June 2026

distribution patterns, with most individuals located within the upper 50 m, particularly in the central region. Average concentrations reached 0.08 cells mL^{-1} (*Discosphaera*) and 0.09 cells mL^{-1} (*Rhabdosphaera*) in SYRACO counts and 0.12 cells mL^{-1} (*Discosphaera*) in manual counts. Manual observations also showed *Rhabdosphaera* extending down to 100 m depth in the central region and slightly higher abundances in the eastern sector.

Calciosolenia was detected along the entire transect in both datasets, with mean concentrations of 0.21 cells mL^{-1} in SYRACO counts and 0.05 cells mL^{-1} in manual counts. Higher abundances occurred near 100 m depth in the eastern region and below 80 m in the central gyre. SYRACO also detected a substantial population near the Marquesas.

Among the Coccolithales, *Umbilicosphaera sibogae* occurred along the entire transect with similar mean concentrations in SYRACO and manual counts (0.19 and 0.17 cells mL^{-1}, respectively), peaking near stations located at the transition between the central gyre and peripheral nutrient-rich regions (100–80° W). Other *Umbilicosphaera* species averaged 0.29 cells mL^{-1} in SYRACO counts and 0.04 cells mL^{-1} in manual counts and were more frequent in nutrient-rich waters, particularly between 0 and 100 m depth in the eastern and western regions, but were scarcely present in the upper euphotic zone (0–50 m) of the central gyre. Other Calcidiscaceae were mainly observed in the eastern and western sectors, with slightly lower abundances in manual counts (0.37 cells mL^{-1}) than in SYRACO counts (0.46 cells mL^{-1}).

Deep-dwelling taxa were primarily observed near the transition between the Marquesas region and the central oligotrophic gyre. *Florisphaera profunda* and *Gladiolithus* occurred predominantly in the lower euphotic zone, with abundance maxima below 150 m in the Marquesas region and below 200 m in the central gyre. Mean concentrations remained low, averaging 0.07 and 0.03 cells mL^{-1} in SYRACO counts and 0.06 and 0.03 cells mL^{-1} in manual counts for *Florisphaera* and *Gladiolithus*, respectively. *Algirosphaera* reached mean concentrations of 0.10 cells mL^{-1} in SYRACO counts and 0.02 cells mL^{-1} in manual counts, with maxima observed in nutrient-rich waters at 25–60 m depth at 134.09° W (SYRACO) and near 105 m depth at 95.45° W (manual counts).

Umbellosphaera represented the third most abundant taxon after *Emiliania* and *Gephyrocapsa*, with mean concentrations of 1.05 cells mL^{-1} in SYRACO counts and 1.13 cells mL^{-1} in manual counts. SYRACO detected *Umbellosphaera* along the entire transect, with higher concentrations in the eastern sector down to 150 m depth. In manual counts, concentrations were higher in the western half of the transect, with maxima observed between 0 and 50 m near the Marquesas and between 50 and 100 m in the central gyre.

Rare taxa included *Helicosphaera* and *Ceratolithus*. *Helicosphaera* averaged 0.02 cells mL^{-1} in SYRACO counts and 0.01 cells mL^{-1} in manual counts and occurred mainly within the upper 100 m in the western region and, to a lesser extent, in the eastern sector. Manual counts recorded *Helicosphaera* between 0 and 50 m near the Marquesas and near 100 m depth in the eastern sector. *Ceratolithus* averaged 0.01 cells mL^{-1} in SYRACO counts and 0.02 cells mL^{-1} in manual counts and was detected intermittently along the transect down to 200 m depth.

3.1.2 Assemblage composition

https://doi.org/10.5194/egusphere-2026-3055
Preprint. Discussion started: 26 June 2026

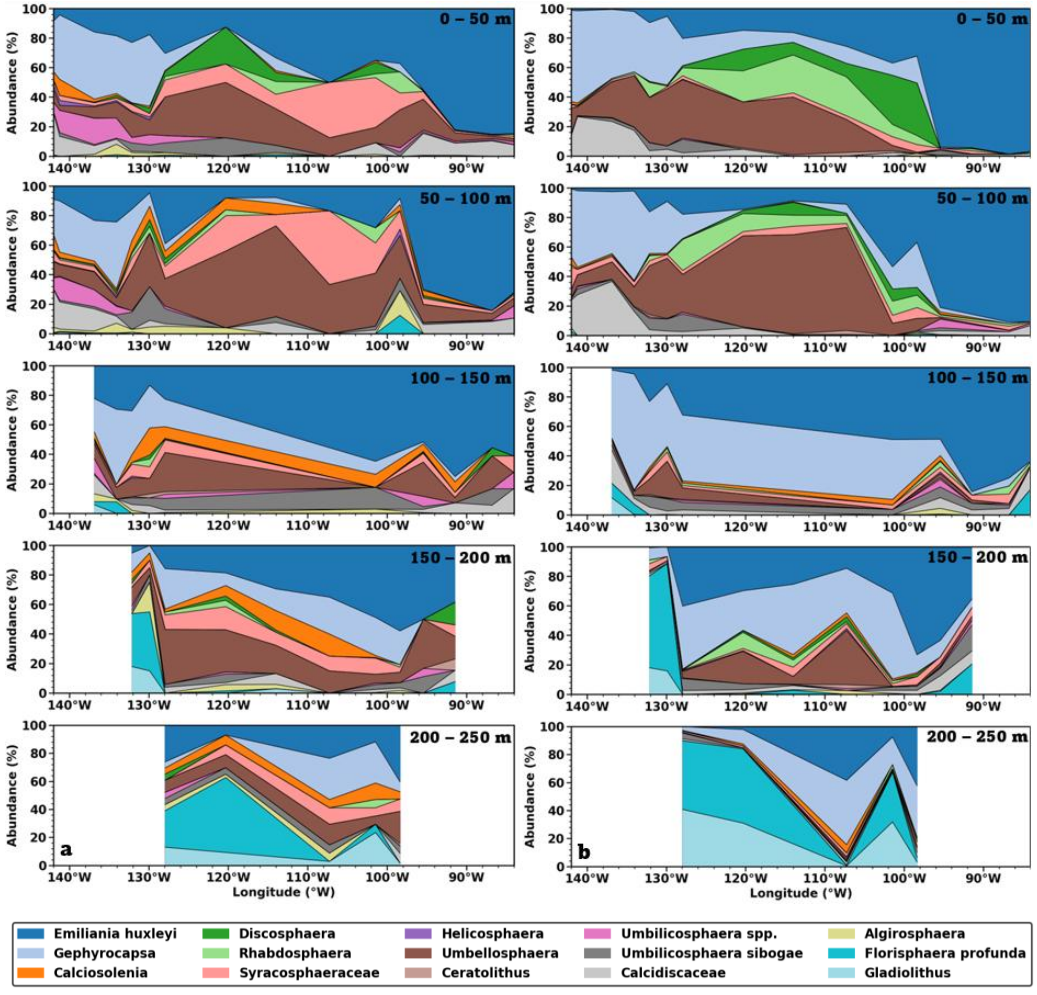

Figure 4 Vertical profile of coccolithophore assemblage composition from the surface to –250 m from **(a)** SYRACO and **(b)** manual-based counts. Relative abundances are calculated in 50 m increments.

Transect-wide, *Emiliania* was the most abundant taxon, accounting for 47.33 % of total integrated abundance in SYRACO counts and 46.38 % in manual counts. Assemblages derived from SYRACO (fig. 4a) exhibited slightly more diversity than those obtained from manual counts (fig. 4b).

Coccolithophore communities in the eastern and western regions were largely dominated by Isochrysidales. Assemblages from the Marquesas were dominated by *Gephyrocapsa* (SYRACO: 35.85 %; manual: 45.87 %), whereas those in the eastern transition region were dominated by *Emiliania* (SYRACO: 77.64 %; manual: 90.59 %). Marquesas assemblages nevertheless showed higher diversity, with a substantial contribution from Calcidiscaceae, including *Umbilicosphaera* spp. (8.01 % in SYRACO). In contrast, communities near the PCU were markedly more homogeneous and strongly dominated by *Emiliania*.

https://doi.org/10.5194/egusphere-2026-3055
Preprint. Discussion started: 26 June 2026

Assemblages in the central gyre were more diverse and vertically structured than in nutrient-rich regions. Between 0 and 230 m depth, the two dominant taxa were *Emiliania* (SYRACO: 28.40 %; manual: 25.18 %) and *Umbellosphaera* (SYRACO: 25.76 %; manual: 29.37 %).

In the upper euphotic layer (0–100 m), assemblages were dominated by *Umbellosphaera*, together with contributions from *Discosphaera*, *Rhabdosphaera*, and Syracosphaeraceae. In the intermediate layer (100–200 m), assemblages remained largely dominated by Isochrysidales, with *Emiliania* dominating SYRACO counts (38.94 %) and *Gephyrocapsa* dominating manual counts (39.5 %). *Umbellosphaera* also represented a substantial component of the assemblages in both datasets (SYRACO: 16.05 %; manual: 7.72 %).

Below 200 m depth, assemblages showed increasing contributions from deep-dwelling taxa and were mainly composed of *Emiliania* (SYRACO: 21.74 %; manual: 18.03 %) and *Florisphaera* (SYRACO: 17.09 %; manual: 28.29 %), together with substantial contributions from *Gephyrocapsa* (SYRACO: 14.04 %; manual: 23.09 %), *Gladiolithus* (SYRACO: 10.11 %; manual: 21.54 %), and *Umbellosphaera* (SYRACO: 12.28 %; manual: 0.32 %). Other taxa remained minor components (<7 %).

Some discrepancies were nevertheless observed between both approaches, notably higher relative abundances of *Umbilicosphaera sibogae* and *Calciosolenia* in the central region in SYRACO results compared with manual counts. Despite these differences, overall assemblage composition derived from SYRACO remained broadly consistent with manual counts.

3.1.3 Statistical analysis

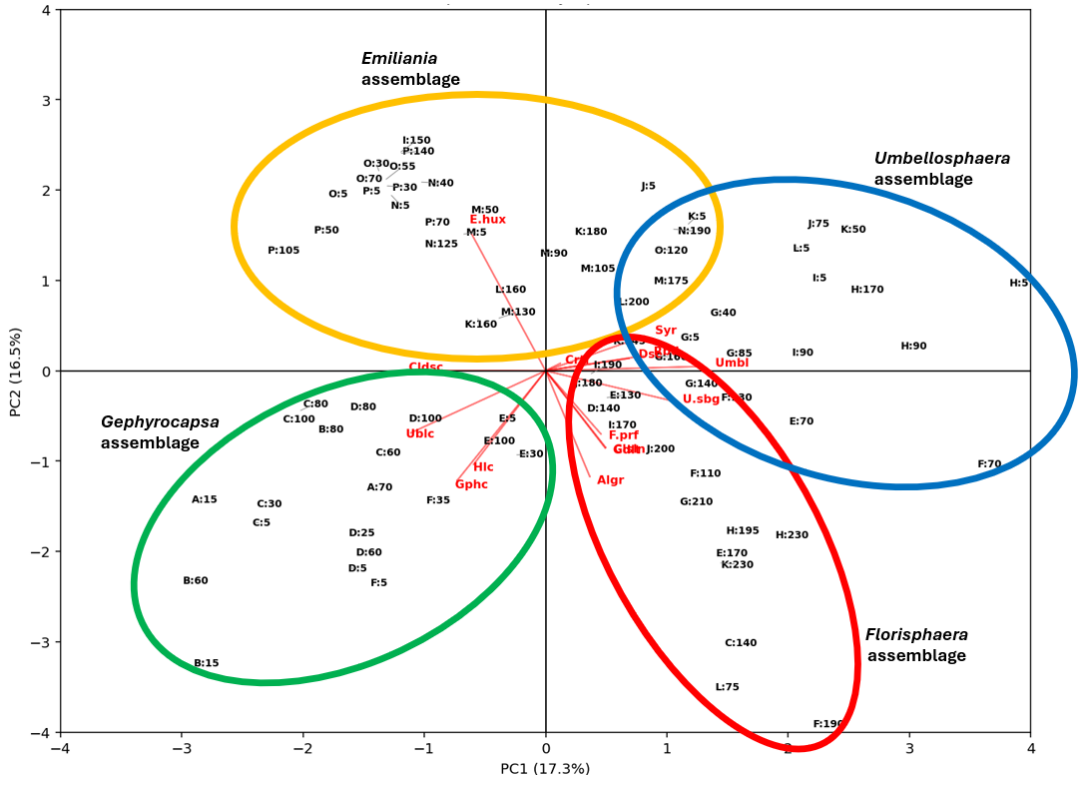

https://doi.org/10.5194/egusphere-2026-3055
Preprint. Discussion started: 26 June 2026

Figure 5 PCA results depicting the position of taxa (red text) and BIOSOPE samples (black text) on the PC1/PC2 plane of the PCA. Model classes abbreviations are: *Algirosphaera* (Algr), *Calciosolenia* (Clsln), *Ceratolithus* (Crtl), *Discosphaera* (Dsc), *Emiliania huxleyi* (E.hux), *Florisphaera profunda* (F.prf), *Gephyrocapsa* (Gphc), *Gladiolithus* (Gdlt), *Helicosphaera* (Hlc), *Rhabdosphaera* (Rbd), Calcidiscaceae (Cldsc), Syracosphaeraceae (Syr), *Umbellosphaera* (Umbl), *Umbilicosphaera* spp. (Ublc), and *Umbilicosphaera sibogae* (U.sbg). BIOSOPE samples are identified by a letter associated to a specific station, in order of sampling (A: SE3, B: MAR1, C: HLN1, D: STB1, E: STB2, F: STB3, G: STB4, H: STB7, I: GYR2, J: STB11, K: STB13, L: STB14, M: STB15, N: EGY2, O: STB17, P: STB18) followed by the sampling depth. Affiliated taxon and samples are highlighted with colored ellipses.

A principal component analysis (PCA) based on taxon-specific concentrations (Fig. 5) revealed a clear regional and vertical structuring of BIOSOPE samples consistent with the assemblage patterns described above.

Samples from the eastern region were primarily associated with *Emiliania*, whereas samples from the western part of the transect showed stronger affinities with *Gephyrocapsa*, *Helicosphaera*, Calcidiscaceae, and *Umbilicosphaera* spp. Samples from the central gyre were mainly associated with *Discosphaera*, Syracosphaeraceae, *Rhabdosphaera*, *Umbellosphaera*, and *Umbilicosphaera sibogae*. Deep samples were characterized by associations with *Algirosphaera*, *Florisphaera*, *Gladiolithus*, and *Calciosolenia*.

Overall, this clustering reflects the major trophic and vertical gradients previously described along the BIOSOPE transect and supports the ecological consistency of the assemblage structure derived from SYRACO.

3.1.4 Pearson correlation analysis

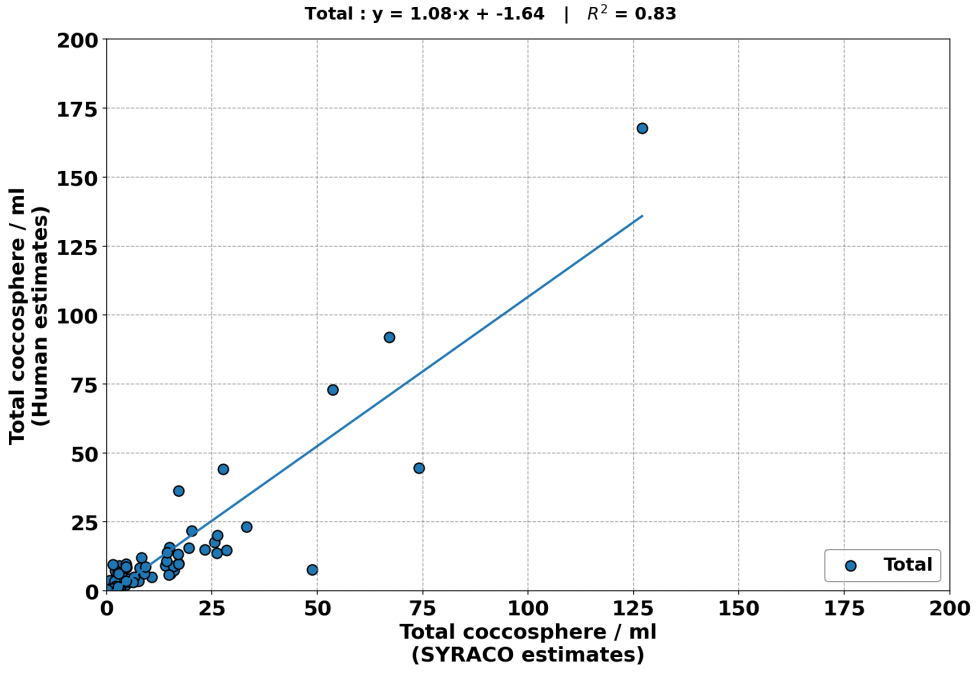

https://doi.org/10.5194/egusphere-2026-3055
Preprint. Discussion started: 26 June 2026

Figure 6 Pearson correlation between human and SYRACO-based total coccolithophore abundance estimates in BIOSOPE samples (blue dots). Regression curve is depicted in blue.

Overall, SYRACO and manual counts showed strong agreement at the transect scale (R = 0.91; slope = 1.08), indicating consistent proportionality between both datasets for total coccosphere abundances (Fig. 6). This agreement was primarily driven by dominant taxa that structure assemblage composition and control most of the coccosphere-associated $CaCO_3$ standing stocks.

At the taxon-specific level, the strongest correlations were observed for Isochrysidales (*Emiliania*: R = 0.93; *Gephyrocapsa*: R = 0.81), together with the deep-dwelling taxa *Florisphaera profunda* (R = 0.84) and *Gladiolithus* (R = 0.87). These taxa represent the main contributors to total coccosphere abundances along the transect and therefore largely determine the overall agreement between both approaches.

Moderate correlations were obtained for *Umbilicosphaera sibogae*, *Calciosolenia*, Calcidiscaceae, and *Rhabdosphaera*, whereas weaker correlations characterized Syracosphaeraceae and *Umbilicosphaera* spp. These differences likely reflect increasing taxonomic complexity and lower abundances compared to dominant taxa.

Very weak correlations were observed for *Umbellosphaera* and *Discosphaera*, and no significant correlation was detected for *Helicosphaera*, *Ceratolithus*, and *Algirosphaera*. These taxa were typically represented by fewer than 10 individuals per sample and were counted using different microscope configurations in the automated and manual approaches. Under such conditions, small absolute counting differences between methods can produce large relative variations, mechanically reducing correlation coefficients without indicating systematic disagreement between datasets.

Despite weak correlations observed for several low-abundance taxa, assemblage composition and regional patterns of coccosphere-associated $CaCO_3$ standing stocks derived from SYRACO remained consistent with those obtained from manual counts. These differences therefore mainly reflect counting variability associated with rare taxa rather than systematic discrepancies between methods.

3.2 Carbonate standing stock

3.2.1 Coccosphere masses and diameters

Table 1 Taxon-specific individual average weight (pg $cell^{-1}$) and diameter (µm $cell^{-1}$), minimum and maximum applied growth rates (d^{-1}) and $CaCO_3$ production rate estimates (pg $CaCO_3$ d^{-1}).

Taxa	Total count	Weight (pg $cell^{-1}$)		Diameter (µm $cell^{-1}$)		Growth rate (d^{-1})			CaCO3 production rate (pg CaCO3 d^{-1})	
		Average	Strd Dev	Average	Strd Dev	Min	Max	Sources	Min	Max
Emiliania huxleyi	8508	22.50 ± 0.49	4.97	5.47 ± 0.04	0.41	**0.6**	**1.4**	**Sett et al. (2014)**	13.50	31.50
Gephyrocapsa	2014	45.11 ± 0.91	9.26	6.38 ± 0.05	0.52	**0.6**	**1.1**	**Sett et al. (2014)**	27.06	49.62
Calciosolenia	308	30.47 ± 3.33	33.92	12.69 ± 0.4	4.08	0.53	0.66	from *S. pulchra* values	16.15	20.11
Discosphaera	148	38.68 ± 2.32	23.71	9.39 ± 0.2	1.99	0.53	0.66	from *S. pulchra* values	20.50	25.53
Rhabdosphaera	147	42.88 ± 2.43	24.82	8.96 ± 0.25	2.55	0.53	0.66	from *S. pulchra* values	22.72	28.30
Syracosphaeraceae	755	80.99 ± 4.16	42.39	11.95 ± 0.24	2.48	**0.53**	**0.66**	**Fiorini et al. (2011)**	42.92	53.45
Helicosphaera	89	176.38 ± 15.21	155.11	9.43 ± 0.35	3.59	**0.36**	**0.44**	**Bianco et al. (2025)**	63.50	77.61

https://doi.org/10.5194/egusphere-2026-3055
Preprint. Discussion started: 26 June 2026

Umbellosphaera	1265	31.47 ± 0.88	9.00	7.87 ± 0.14	1.48	0.15	0.15	from *C. leptoporus* values	4.72	4.72
Ceratolithus	13	77.67 ± 3.64	37.11	12.00 ± 0.31	3.16	0.15	0.15	from *C. leptoporus* values	11.65	11.65
Umbilicosphaera spp.	576	151.88 ± 4.84	49.35	9.30 ± 0.12	1.22	0.15	0.61	from *C. leptoporus* values	22.78	92.65
Umbilicosphaera sibogae	221	189.03 ± 9.23	94.13	16.38 ± 0.41	4.22	0.15	0.61	from *C. leptoporus* values	28.35	115.31
Calcidiscaceae	1120	44.53 ± 2.07	21.08	5.49 ± 0.08	0.77	**0.15**	**0.61**	**Diner et al. (2015)**	6.68	27.16
Algirosphaera	159	61.55 ± 3.56	36.35	8.51 ± 0.14	1.46	0.15	0.15	from *C. leptoporus* values	9.23	9.23
Florisphaera Profunda	122	23.39 ± 0.97	9.88	5.34 ± 0.1	1.02	0.15	0.15	from *C. leptoporus* values	3.51	3.51
Gladiolithus	62	30.61 ± 2.31	23.59	7.54 ± 0.16	1.60	0.15	0.15	from *C. leptoporus* values	4.59	4.59

At the scale of the entire transect, coccosphere masses varied markedly between major taxonomic groups (Table 1). Within the Isochrysidales, *Gephyrocapsa* exhibited higher average coccosphere mass (45.11 ± 0.91 pg) than *Emiliania* (22.5 ± 0.49 pg), although both taxa displayed similar coccosphere diameters (5.47 ± 0.04 µm and 6.38 ± 0.05 µm, respectively) and limited variability.

Among the Syracosphaerales, Syracosphaeraceae showed the highest average coccosphere mass (80.99 ± 4.16 pg), whereas *Calciosolenia* exhibited the lowest values (30.47 ± 3.33 pg). Despite its lower mass, *Calciosolenia* displayed a larger average diameter (12.69 ± 0.40 µm) than Syracosphaeraceae (11.95 ± 0.24 µm), reflecting its elongated coccosphere morphology. *Discosphaera* and *Rhabdosphaera* showed similar morphometric characteristics, with comparable masses (38.68 ± 2.32 pg and 42.88 ± 2.43 pg) and diameters (9.39 ± 0.2 µm and 8.96 ± 0.25 µm).

Within the Coccolithales, *Umbilicosphaera* displayed the highest coccosphere masses of all taxa analysed, reaching 151.88 ± 4.84 pg for *Umbilicosphaera* spp. and 189.03 ± 9.23 pg for *U. sibogae*. Coccosphere diameter averaged 9.30 ± 0.12 µm and 16.38 ± 0.41 µm, respectively, with particularly strong variability observed in *U. sibogae*. Other Calcidiscaceae exhibited lower average masses (44.53 ± 2.07 pg) and smaller diameters (5.49 ± 0.08 µm).

Among deep-dwelling taxa, *Algirosphaera* displayed the highest values (61.55 ± 3.56 pg; 8.51 ± 0.14 µm), whereas *Florisphaera* and *Gladiolithus* showed lower average masses (23.39 ± 0.97 pg and 30.61 ± 2.31 pg) and smaller diameters (5.34 ± 0.10 µm and 7.54 ± 0.16 µm), with limited morphometric variability.

Umbellosphaera exhibited intermediate coccosphere mass (31.47 ± 0.88 pg) and diameter (7.87 ± 0.14 µm), whereas *Ceratolithus* showed higher values (77.67 ± 3.64 pg; 12.00 ± 0.31 µm). *Helicosphaera* displayed one of the highest coccosphere masses among all taxa studied (176.38 ± 15.21 pg), despite being represented by relatively few individuals.

3.2.2 $CaCO_3$ distribution

https://doi.org/10.5194/egusphere-2026-3055
Preprint. Discussion started: 26 June 2026

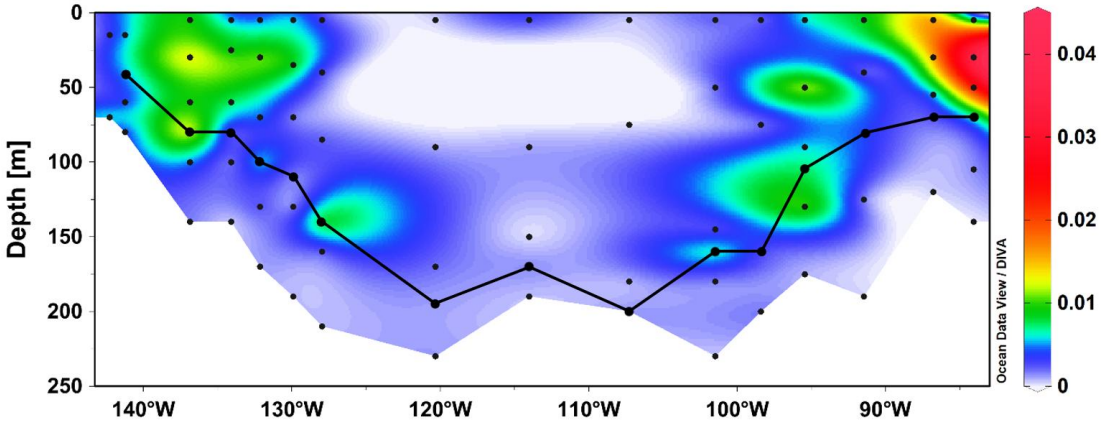

Figure 7 $CaCO_3$ stock (mmol m^{-3}) vertical distribution along sampled depth (black dots) of the BIOSOPE transect. The black line represents the DCM based on Claustre et al (2008).

The total calcite standing stock represented by coccospheres reached approximately 3.47×10^6 mmol m^{-1} along the entire transect corresponding to an average of 515×10^{-3} mmol m^{-2}. The highest calcite standing stocks were observed in nutrient-rich regions (Fig. 7), reaching on average 677×10^{-3} mmol m^{-2} offshore of the Marquesas Archipelago and 801×10^{-3} mmol m^{-2} in the eastern transition region. Although lower, a substantial calcite stock was also present in the oligotrophic central gyre (~300×10^{-3} mmol m^{-2}).

In the western and eastern regions, most of the carbonate stock was concentrated in the upper euphotic layer, with maximum densities between 0 and 50 m depth. In contrast, in the central gyre, calcite standing stocks were primarily located in the intermediate (100–200 m) and deep (200–230 m) layers of the euphotic zone, where the $CaCO_3$ maximum generally coincided with the DCM, typically located between 150 and 200 m.

Across the transect, nutrient-rich regions accounted for most of the total calcite standing stock (Marquesas: 38.07 %; eastern region: 45.08 %), whereas the central gyre contributed only ~16.86 %.

3.2.3 Taxon-specific carbonate stocks

https://doi.org/10.5194/egusphere-2026-3055
Preprint. Discussion started: 26 June 2026

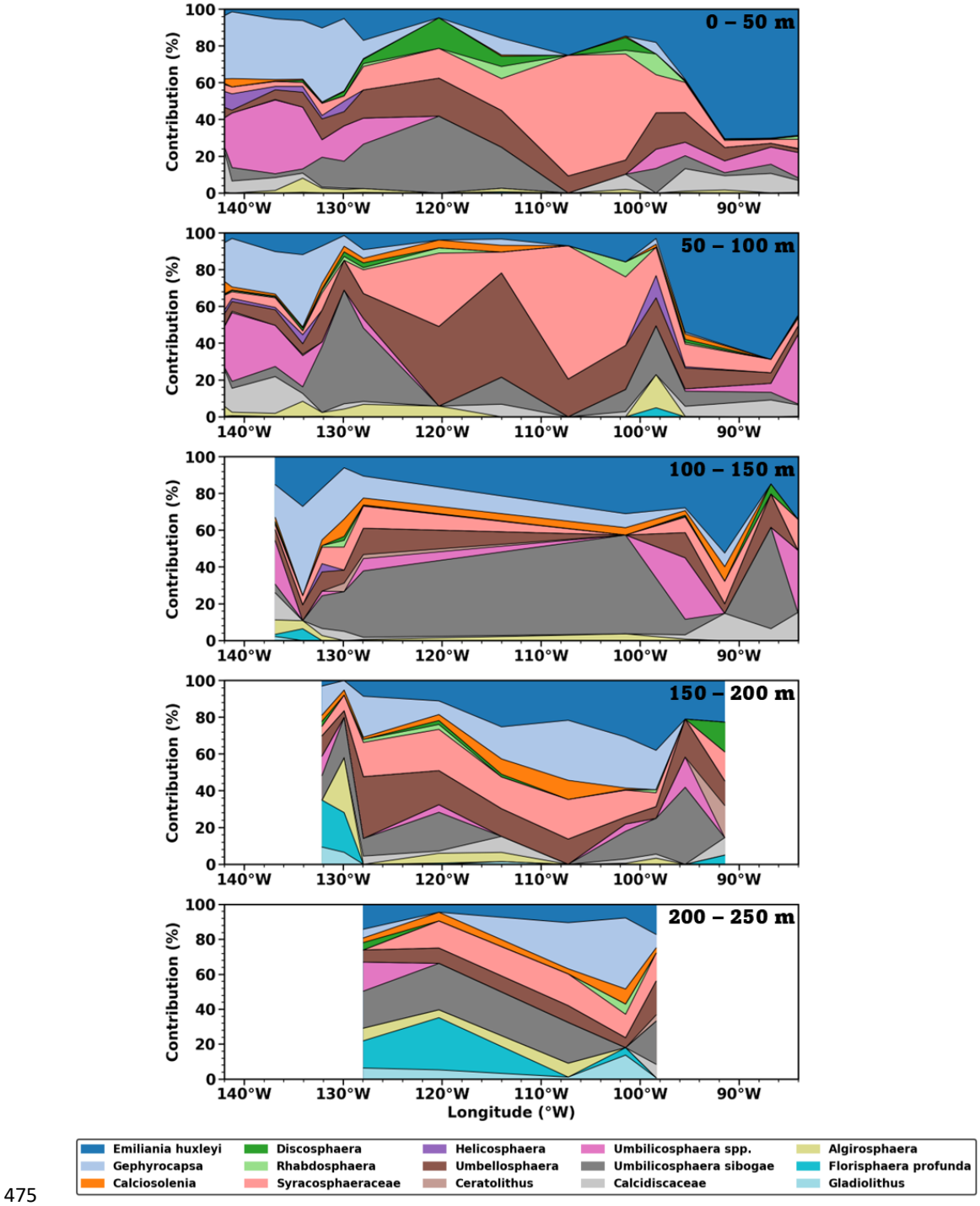

Figure 8 Vertical profile of Coccolithophore contribution (%) to Calcite stocks from the surface to –250 m. Relative contributions are calculated in 50 m increments.

https://doi.org/10.5194/egusphere-2026-3055
Preprint. Discussion started: 26 June 2026

Among the various taxa, *Emiliania* accounted for the largest fraction of the total calcite standing stock at the transect scale (129×10^{-3} mmol m^{-2} or 24.99 %) (Fig. 8). However, at the regional scale, $CaCO_3$ stocks were primarily driven by locally dominant taxa.

Near the Marquesas Archipelago, most of the calcite stock was contributed by *Gephyrocapsa* (30.39 %), whereas in the eastern region near the PCU, *Emiliania* largely dominated carbonate standing stocks (57.62 %). Despite its low abundance in global assemblages (3.76 %), *Umbilicosphaera* spp. substantially contributed to the $CaCO_3$ stock in nutrient-rich regions (Marquesas: 21.95 %; eastern region: 13.88 %).

In the central region of the transect, carbonate standing stocks were shared among a broader diversity of taxa, with major contributions from Syracosphaeraceae (19.65 %), *Umbellosphaera* (19.08 %), *Umbilicosphaera sibogae* (21.51 %), and, to a lesser extent, *Emiliania* (14.53 %).

As observed for abundances, taxon-specific contributions to calcite standing stocks also varied vertically along the water column. In the upper euphotic layer (0–100 m), most of the calcite stock was contributed by Syracosphaeraceae (31.69 %) and *Umbellosphaera* (22.17 %), with additional contributions from *U. sibogae* (16.23 %) and *Emiliania* (11.39 %). Although abundant in surface waters, *Discosphaera* and *Rhabdosphaera* contributed only minor fractions of the calcite stock in this layer (2.85 % and 2.79 %, respectively).

In the intermediate euphotic layer (100–200 m), *U. sibogae* was the dominant contributor to the calcite stock (27.89 %). Isochrysidales also accounted for a substantial fraction (*Emiliania*: 21.63 %; *Gephyrocapsa*: 15.64 %), while the remaining stock was mainly represented by Syracosphaeraceae (11.52 %) and *Umbellosphaera* (11.18 %).

In the deep euphotic layer (200–230 m), the calcite stock was again largely dominated by *U. sibogae* (19.16 %), with additional contributions from Syracosphaeraceae (12.62 %), *Gephyrocapsa* (15.97 %), *Emiliania* (10.76 %), and *Umbellosphaera* (10.09 %). Deep-dwelling taxa together accounted for 19.36 % of the total carbonate stock (*Florisphaera profunda*: 9.95 %; *Gladiolithus*: 5.47 %; *Algirosphaera*: 3.93 %).

3.2.4 $CaCO_3$ production rates estimates

https://doi.org/10.5194/egusphere-2026-3055
Preprint. Discussion started: 26 June 2026

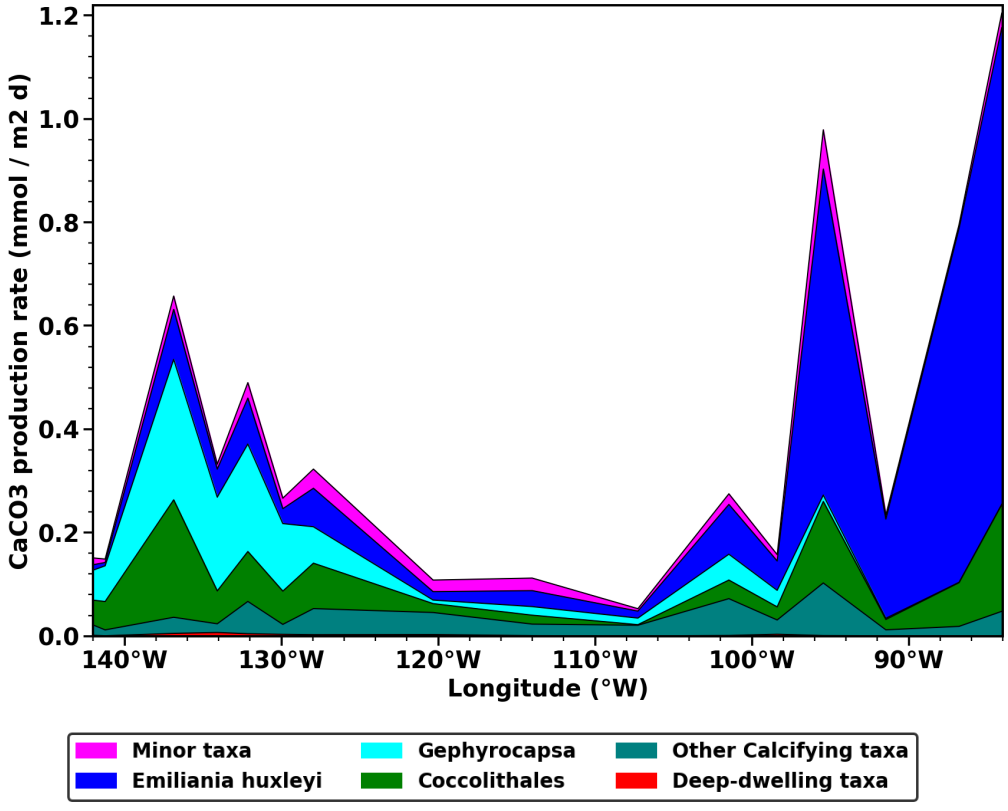

Figure 9 $CaCO_3$ production rate estimates (mmol m^{-2} d^{-1}) along the BIOSOPE transect. Minor taxa include *Calciosolenia*, *Discosphaera*, *Rhabdosphaera*, *Umbellosphaera* and *Ceratolithus*. Coccolithales is comprised of *Umbilicosphaera* spp., *Umbilicosphaera sibogae* and Calcidiscaceae. Other Calcifying taxa include Syracosphaeraceae and *Helicosphaera*. Deep-dwelling taxa is comprised of *Algirosphaera*, *Florisphaera* and *Gladiolithus*).

Estimated coccolithophore $CaCO_3$ production along the transect ranged between 1.39×10^6 and 2.96×10^6 mmol m^{-1} d^{-1}, corresponding to average values between 0.21 and 0.44 mmol m^{-2} d^{-1} (Fig. 9).

The highest $CaCO_3$ production rates were observed in the eastern region (~54.19 % of total production), largely dominated by *Emiliania* (77.66 %). Offshore of the Marquesas (~32.6 %), production was mainly driven by *Gephyrocapsa* (46.06 %), with an additional contribution from *Umbilicosphaera* spp. (15.81 %) (Table 1 and 2).

Although lower, the contribution from SPG communities (~13.2 %) remained substantial and involved a broader diversity of taxa, including Syracosphaeraceae (26.14 %), *Emiliania huxleyi* (25.08 %), *Gephyrocapsa* (17.01 %), and *U. sibogae* (12.56 %). However, these estimates should be considered first-order approximations, as growth rates applied to *Umbellosphaera* and deep-dwelling taxa—dominant in the upper and deep euphotic layers of the central gyre—were based on the minimal growth rate reported for *Calcidiscus leptoporus*.

Because taxon-specific growth rates remain poorly constrained under the contrasted environmental conditions encountered along the transect, the reliability of production estimates likely varies among taxa. Nevertheless,

https://doi.org/10.5194/egusphere-2026-3055
Preprint. Discussion started: 26 June 2026

estimated production rates for individual *Emiliania huxleyi* and *Helicosphaera carteri* fall within the range reported in previous studies, with values between 6 and 20 pg $CaCO_3$ $cell^{-1}$ d^{-1} for *Emiliania*, and slightly below the lower threshold of ~80 pg $CaCO_3$ $cell^{-1}$ d^{-1} for *Helicosphaera* (De Bodt et al., 2010; Langer et al., 2009; Šupraha et al., 2015, cited in Bianco et al., 2025a).

Table 2 Absolute and relative calcite concentrations (mmol m^{-2}) and production estimates (mmol m^{-2} d^{-1}) at the transect and specific regional scale.

Region	CaCO3 Standing Stock		CaCO3 Production Estimates		
	Average (mmol m^{-2})	%	Average (mmol m^{-2} d^{-1}) Min	Max	%
Full transect	0.51	-	0.21	0.44	-
Marquesas	0.68	38.07	0.25	0.54	32.60
SPG	0.3	16.86	0.11	0.2	13.20
East	0.8	45.08	0.4	0.93	54.19

4 Discussion

4.1 SYRACO performance and biases

Overall, the new SYRACO iteration proved robust for quantifying coccolithophore abundances at the transect scale. Total coccosphere concentrations showed strong agreement with manual counts (R = 0.91 with a regression slope nearing unity y = 1.08), indicating that the automated workflow reproduces absolute abundance estimates with high accuracy. Because these total concentrations integrate the contribution of all taxa across the water column, this result demonstrates the reliability of SYRACO for reconstructing the large-scale structure of coccolithophore populations along the BIOSOPE transect.

At the taxonomic level, the strongest agreement with manual counts was obtained for the dominant taxa structuring coccolithophore assemblages, particularly Isochrysidales (*Emiliania* and *Gephyrocapsa*) and the main deep-dwelling taxa (*Florisphaera profunda* and *Gladiolithus*). These groups represent the largest contribution to both total coccosphere abundances and coccosphere-associated $CaCO_3$ standing stocks, so their accurate detection is critical for the quantitative objectives of this study. Their high correlations with manual counts therefore confirm the robustness of the automated approach for the taxa that control most of the carbonate inventory along the transect.

More generally, SYRACO-derived assemblages reproduced the main regional and vertical ecological gradients observed along the BIOSOPE transect. This consistency is further supported by the PCA, which shows that automated counts correctly capture the ecological structuring of coccolithophore communities across the Marquesas region, the eastern transition zone, and the oligotrophic South Pacific Gyre. These results indicate that SYRACO reliably reconstructs the spatial organization of coccolithophore assemblages at the ecosystem scale.

Lower correlations observed for several secondary taxa mainly reflect their low abundances rather than systematic disagreement between automated and manual counts. When fewer than ~10 individuals are detected per sample, small absolute counting differences between methods mechanically produce large relative variations and therefore reduce correlation coefficients. In most cases, these taxa were consistently identified as rare by both approaches,

https://doi.org/10.5194/egusphere-2026-3055
Preprint. Discussion started: 26 June 2026

indicating good agreement in absolute terms despite weak statistical correlations. Because these taxa contribute only marginally to total coccosphere abundances and carbonate standing stocks, their limited statistical agreement has little influence on the reconstruction of assemblage structure or $CaCO_3$ inventories.

Some remaining discrepancies between SYRACO and manual counts appear to reflect methodological differences related to imaging conditions. In particular, *Emiliania* abundances were systematically higher in manual counts in the eastern sector. SYRACO may underestimate coccospheres occurring within aggregates because only peripheral individuals are reliably resolved, whereas manual counts may include overlapping specimens. This effect was particularly evident in sample STB18_4, where slight filter deformation generated focal heterogeneity and likely reduced the detection of small *E. huxleyi*. Conversely, discrepancies observed for *Gephyrocapsa* in sample STB13_3 may partly reflect slight overestimation in manual counts, as SYRACO results were supported by independent manual annotation performed directly on the corresponding images.

Taxon-specific morphological characteristics also contributed to the observed variability. SYRACO showed good agreement with manual counts for taxa with distinctive morphologies such as *Calciosolenia* and *Umbilicosphaera sibogae*, although fragmented coccospheres of *Calciosolenia* may occasionally be interpreted as multiple individuals. Lower correlations for Calcidiscaceae, Syracosphaeraceae, *Rhabdosphaera*, *Discosphaera*, and *Umbellosphaera* likely reflect a combination of limited representation in the training dataset, preservation state of coccospheres in BIOSOPE samples, and differences in visibility between imaging modes. In particular, some Syracosphaerales such as *Michaelsarsia* are less visible under linear polarization and may therefore be underestimated in manual counts, whereas bidirectional circular polarization combined with grey-level analysis improves their detection in SYRACO outputs.

Finally, the absence of correlation for *Algirosphaera*, together with its occasional occurrence in unexpected shallow samples in SYRACO outputs, suggests residual misclassification during inferences, possibly involving confusion and ensuing false positives. However, these rare discrepancies do not significantly affect the reconstruction of regional assemblage structure or coccosphere-associated carbonate standing stocks, which remain broadly consistent between SYRACO and manual counts.

4.2 Ecological structure of Coccolithophores communities:

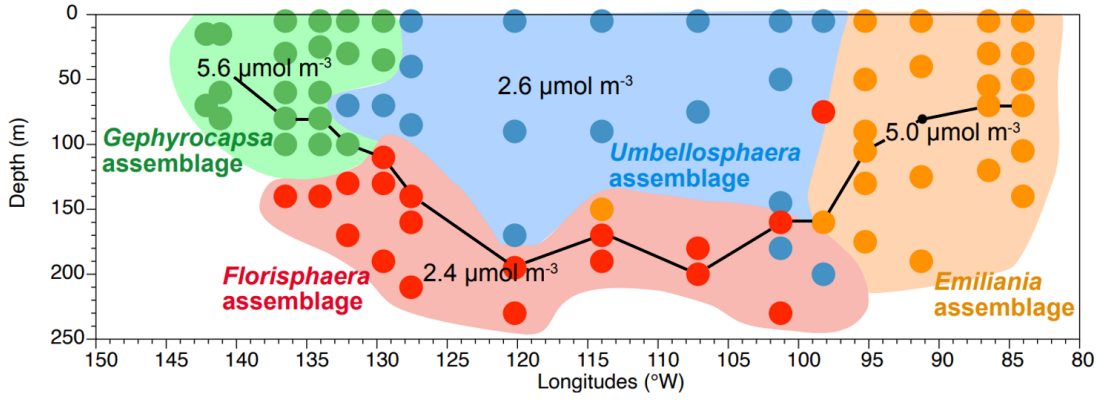

https://doi.org/10.5194/egusphere-2026-3055
Preprint. Discussion started: 26 June 2026

Figure 10 Mean coccosphere-associated $CaCO_3$ concentrations across major South Central Pacific coccolithophore assemblages. Depicted concentrations are calculated based on same-colored samples. The black line represents the DCM based on Claustre et al (2008).

Because SYRACO and manual counts showed strong agreement across the transect, the resulting assemblages provide a reliable basis for ecological interpretation. Coccolithophore communities followed the expected trophic gradient between the productive western sector near the Marquesas Archipelago, the eastern transition zone toward the Peru–Chile Upwelling, and the strongly stratified oligotrophic waters of the South Pacific Gyre (SPG). Coccosphere concentrations remained within the range reported for other subtropical gyres, including the North Pacific Subtropical Gyre (Han et al., 2025), supporting the representativeness of the observed distributions.

In nutrient-rich and transitional regions, assemblages were largely dominated by Isochrysidales, particularly *Gephyrocapsa* near the Marquesas and *Emiliania huxleyi* in the eastern sector, consistent with previous descriptions of the BIOSOPE transect (Beaufort et al., 2008). Such dominance is in agreement with the well-known affinity of opportunistic Isochrysidales for nutrient-enriched and weakly stratified environments (Okada and Honjo, 1973; Tyrrell and Merico, 2004; Baumann et al., 2008; Poulton et al., 2017; Keuter et al., 2022; Guerreiro et al., 2023; Han et al., 2025).

In contrast, assemblages in the SPG were more vertically structured and taxonomically diverse, reflecting strong water-column stratification and reduced nutrient supply in surface waters. The upper euphotic layer was dominated by *Umbellosphaera* together with Syracosphaeraceae and *Rhabdosphaera*, taxa typically associated with warm, stratified, oligotrophic environments (Hagino et al., 2000; Baumann et al., 2008; Keuter et al., 2022; Han et al., 2025). In deeper layers, *Florisphaera profunda*, *Gladiolithus*, and *Algirosphaera* became increasingly abundant, consistent with their recognized affinity for the lower euphotic zone in oligotrophic systems (Okada and Honjo, 1973; Beaufort et al., 2008; Dimiza et al., 2016; Poulton et al., 2017; Guerreiro et al., 2023).

The marked concentration of Isochrysidales near the DCM further supports the view that this depth horizon represents a major ecological niche for coccolithophores in stratified subtropical gyres (Baumann et al., 2008; Beaufort et al., 2008; Keuter et al., 2022). The distribution of *U. sibogae* further confirms its affinity for oligotrophic environments (Okada and Honjo, 1975; Giraudeau, 1992 cited in Baumann et al., 2008), whereas *Umbilicosphaera* spp. appeared preferentially associated with more productive waters. Altogether, these results highlight strong ecological compartmentalization of coccolithophore communities along the BIOSOPE transect, controlled primarily by trophic gradients and water-column stratification. This organization is synthesized in Fig. 10, where the PCA-derived assemblages closely follow depth and trophic structure, with the *F. profunda* assemblage occurring predominantly below ~150 m, in agreement with Okada and Honjo (1973).

4.3 Carbonate standing stocks

The spatial organization of coccosphere-associated $CaCO_3$ stocks across the BIOSOPE transect reveals a strong coupling between carbonate inventories and large-scale trophic structure, but also a marked decoupling from coccosphere abundance under oligotrophic conditions. In productive regions near the Marquesas Archipelago and the eastern transition zone, carbonate maxima largely coincided with coccolithophore abundance maxima in the upper euphotic zone, reflecting enhanced nutrient availability and elevated coccolithophore standing stocks. In contrast, within the strongly stratified South Pacific Gyre (SPG), carbonate maxima systematically occurred deeper than

https://doi.org/10.5194/egusphere-2026-3055
Preprint. Discussion started: 26 June 2026

abundance maxima and generally coincided with the DCM (Claustre et al., 2008), indicating that carbonate accumulation is tightly linked to subsurface productivity and ecological stratification.

Despite its strongly oligotrophic character, the SPG contributed a substantial fraction of the transect-wide coccosphere-associated carbonate inventory, emphasizing the potential role of highly stratified gyres in basin-scale carbonate budgets. Similar moderate contrasts between productive transition zones and subtropical gyres have been reported in the North Pacific (Han et al., 2025), although the absolute carbonate stocks estimated here remain slightly lower. This difference likely reflects both the stronger oligotrophic character of the southeastern Pacific and methodological differences, as the present estimates are restricted to intact coccospheres and exclude detached coccoliths, which may represent an important component of suspended particulate carbonate.

Taxon-specific contributions further demonstrate that coccolithophore carbonate inventories are not linearly related to coccosphere abundances. While *Emiliania huxleyi* dominated transect-scale carbonate stocks primarily through its numerical abundance, several heavily calcified taxa, particularly *Umbilicosphaera* spp., *U. sibogae*, and Syracosphaeraceae, contributed disproportionately relative to their cell densities because of their high coccosphere calcite content. This highlights the importance of accounting for interspecific calcification differences when estimating pelagic carbonate inventories.

Conversely, deep-dwelling taxa such as *Florisphaera profunda* and *Gladiolithus* contributed only modestly to suspended carbonate stocks despite their ecological importance in the lower euphotic zone. This contrasts with sedimentary assemblages from oligotrophic regions, where *F. profunda* frequently dominates both coccolith abundance and carbonate contribution (Beaufort et al., 1997; Hernández-Almeida et al., 2018; Beaufort et al., 2022). Such discrepancy may reflect enhanced export efficiency and preservation of coccoliths produced near the DCM, or reduced remineralization compared with surface-produced taxa.

More broadly, the coccosphere-based carbonate estimates obtained here highlight the value of bidirectional circular polarization (BCP) imaging for direct taxon-resolved carbonate quantification. Unlike coccolith morphometric approaches based on detached coccoliths, this method directly estimates coccosphere-scale calcite content and therefore better captures the biological structure of carbonate standing stocks. The consistency of BCP-derived coccosphere masses for *Emiliania* and *Gephyrocapsa* with independent experimental estimates (Yang et al., 2022) further supports the reliability of this approach.

4.4 Carbonate production estimates

First-order estimates of coccolithophore $CaCO_3$ production broadly followed the spatial organization of coccosphere-associated carbonate standing stocks, with the highest production occurring in productive regions and lower but sustained production within the oligotrophic SPG. The dominant contribution of *Emiliania huxleyi* in the eastern sector and *Gephyrocapsa* near the Marquesas further confirms the central role of Isochrysidales in carbonate production under nutrient-enriched conditions (Fig. 10).

Despite low surface productivity, the SPG still represented a substantial contribution to transect-scale carbonate production, suggesting that strongly stratified subtropical gyres may constitute persistent carbonate-producing systems at basin scale. Similar limited contrasts between productive transition zones and oligotrophic gyres have been reported in the North Pacific (Han et al., 2025), although production estimates obtained here remain lower, likely reflecting both environmental differences between the southeastern and northwestern Pacific and methodological differences in growth-rate assumptions.

https://doi.org/10.5194/egusphere-2026-3055
Preprint. Discussion started: 26 June 2026

Nevertheless, these production estimates should be interpreted cautiously. Applied growth rates derive from laboratory cultures performed under nutrient-replete and light-saturated conditions and therefore likely overestimate in situ production, particularly in oligotrophic waters and in the lower euphotic zone. Furthermore, growth rates had to be generalized across several taxonomic groups for which no species-specific data are available. Consequently, the estimates presented here should be regarded as first-order potential production rather than direct measurements of calcification rates.

Despite these limitations, the present approach provides the first multispecific estimate of coccolithophore carbonate production across the southeastern Pacific at transect scale. More importantly, it enables quantitative comparison of the relative contributions of major taxonomic groups and trophic regimes to pelagic carbonate cycling, offering a framework for future integration of in situ growth rates and detached coccolith contributions.

5 Conclusion

This study provides the first multispecific assessment of coccosphere-associated $CaCO_3$ standing stocks and first-order production estimates along the BIOSOPE transect in the southeastern Pacific, using an upgraded SYRACO framework combined with bidirectional circular polarization (BCP) imaging. The automated recognition workflow produced results consistent with manual counts and previously described assemblage structures, capturing the major trophic and vertical gradients across one of the strongest productivity contrasts of the global ocean.

At the transect scale, carbonate standing stocks were primarily structured by large-scale trophic gradients, with maxima located in surface waters of nutrient-rich regions offshore of the Marquesas Archipelago and in the eastern transition zone. In contrast, in the South Pacific Gyre, $CaCO_3$ maxima systematically coincided with the DCM, indicating a vertical decoupling between coccosphere abundance and carbonate inventories and highlighting the strong coupling between calcification and subsurface productivity under stratified conditions. Despite its oligotrophic character, the gyre contributed a substantial fraction of the transect-scale carbonate inventory, emphasizing the non-negligible role of stratified oceanic regions in basin-scale pelagic carbonate budgets.

Taxon-specific analyses further demonstrate that carbonate inventories are not solely controlled by coccosphere abundances but also by strong interspecific differences in coccosphere calcite content. While Isochrysidales, particularly *Emiliania huxleyi*, dominated carbonate stocks through their numerical abundance, several more heavily calcified taxa contributed disproportionately relative to their densities. Conversely, deep-dwelling taxa, although structuring assemblages in the lower euphotic zone, represented only a minor fraction of suspended carbonate stocks in the water column. This contrast with their major contribution to sedimentary assemblages in oligotrophic regions suggests differences in production depth and transfer efficiency between surface and deep photic communities.

First-order production estimates followed spatial patterns similar to those observed for standing stocks, with enhanced carbonate production in mesotrophic regions and a sustained contribution from oligotrophic communities. Although these estimates remain constrained by uncertainties related to species-specific growth rates and environmental variability, they provide the first multispecific constraints on taxon-resolved calcification dynamics in the southeastern Pacific.

Overall, this study demonstrates that combining automated coccosphere recognition with direct coccosphere-scale carbonate measurements using BCP imaging provides a robust framework for resolving the taxonomic structure of pelagic carbonate inventories. This approach represents an important step toward quantitative, species-resolved

https://doi.org/10.5194/egusphere-2026-3055
Preprint. Discussion started: 26 June 2026

assessments of coccolithophore contributions to oceanic carbonate cycling across major trophic gradients of the global ocean.

Data Availability

All datasets used in this study are available at Zenodo (DOI: https://doi.org/10.5281/zenodo.20419476). The Supplement includes a station distance matrix for the BIOSOPE transect.

Author contributions

G.L., L.B., M.C., and D.M. conceived and designed the study. G.L., L.B., and M.C. contributed to data acquisition and analysis. G.L. and L.B. wrote the first draft of the manuscript. All authors contributed to data interpretation, revised the manuscript, and approved the final version.

Competing interests

The authors declare that they have no conflict of interests.

Acknowledgements

We thank the captains, crews, and scientific teams involved in the BIOSOPE and CARACALHIS cruises aboard the R/V *Atalante* for their invaluable support during sampling. We are grateful to Alexander Nistor for his assistance on the software tools used on the CEREGE MANTA platform. During manuscript preparation, the authors used OpenAI ChatGPT for language editing and drafting assistance. All outputs were critically reviewed, modified, and validated by the authors, who take full responsibility for the final content.

Financial support

This work was supported by a CIFRE PhD fellowship (CIFRE n°2022/0251) funded by the Association Nationale de la Recherche et de la Technologie (ANRT) and carried out in partnership with the company ZORTH.

References

Alam, M. M., and Islam, M. T.: Machine learning approach of automatic identification and counting of blood cells. Healthcare technology letters, 6(4), 103-108. https://doi.org/10.1049/htl.2018.5098, 2019.

Archer, D. E.: An atlas of the distribution of calcium carbonate in sediments of the deep sea. Global Biogeochemical Cycles, 10(1), 159-174. https://doi.org/10.1029/95gb03016, 1996.

Balch, W. M., Bowler, B. C., Drapeau, D. T., Lubelczyk, L. C., and Lyczkowski, E.: Vertical distributions of coccolithophores, PIC, POC, biogenic Silica, and chlorophyll a throughout the global ocean. Global Biogeochemical Cycles, 32(1), 2-17. https://doi.org/10.1002/2016gb005614, 2018.

https://doi.org/10.5194/egusphere-2026-3055
Preprint. Discussion started: 26 June 2026

Balch, W. M., Drapeau, D. T., Bowler, B. C., and Booth, E. S.: Prediction of pelagic calcification rates using satellite measurements. Deep Sea Research Part II Topical Studies In Oceanography, 54(5-7), 478–495. https://doi.org/10.1016/j.dsr2.2006.12.006, 2007.

Battaglia, G., Steinacher, M., and Joos, F.: A probabilistic assessment of calcium carbonate export and dissolution in the modern ocean. Biogeosciences, 13(9), 2823-2848. https://doi.org/10.5194/bg-13-2823-2016, 2016.

Baumann, K. H., Boeckel, B., and Cepek, M.: Spatial distribution of living coccolithophores along an east- west transect in the subtropical South Atlantic. Journal Of Nannoplankton Research, 30(1), 9-21. https://doi.org/10.58998/jnr2014, 2008.

Baumann, K.-H., Böckel, B., Donner, B., Gerhardt, S., Henrich, R., Vink, A., Volbers, A., Willems, H., and Zonneveld, K. A. F.: Contribution of Calcareous Plankton Groups to the Carbonate Budget of South Atlantic Surface Sediments, in: The South Atlantic in the Late Quaternary, Springer Berlin Heidelberg, Berlin, Heidelberg, 81–99. https://doi.org/10.1007/978-3-642-18917-3_5, 2003.

Beaufort, L.: Weight estimates of coccoliths using the optical properties (birefringence) of calcite. Micropaleontology, 51(4), 289-297. https://doi.org/10.2113/gsmicropal.51.4.289, 2005.

Beaufort, L., Barbarin, N., and Gally, Y.: Optical measurements to determine the thickness of calcite crystals and the mass of thin carbonate particles such as coccoliths. Nature Protocols, 9(3), 633-642. https://doi.org/10.1038/nprot.2014.028, 2014.

Beaufort, L., Couapel, M., Buchet, N., Claustre, H., and Goyet, C.: Calcite production by coccolithophores in the southeast Pacific Ocean. Biogeosciences, 5(4), 1101-1117. https://doi.org/10.5194/bg-5-1101-2008, 2008.

Beaufort, L. and Dollfus, D.: Automatic recognition of coccolith by dynamical neural network. Marine Micropaleontology, 51(1–2), 57–73. https://doi.org/10.1016/j.marmicro.2003.09.003, 2004.

Beaufort, L., Gally, Y., Suchéras-Marx, B., Ferrand, P., and Duboisset, J.: Technical note: A universal method for measuring the thickness of microscopic calcite crystals, based on bidirectional circular polarization. Biogeosciences, 18, 775–785. https://doi.org/10.5194/bg-18-775-2021, 2021.

Beaufort, L., Bolton, C. T., Sarr, A., Suchéras-Marx, B., Rosenthal, Y., Donnadieu, Y., Barbarin, N., Bova, S., Cornuault, P., Gally, Y., Gray, E., Mazur, J., and Tetard, M.: Cyclic evolution of phytoplankton forced by changes in tropical seasonality. Nature, 601(7891), 79-84. https://doi.org/10.1038/s41586-021-04195-7, 2022.

Beaufort, L., and Heussner, S.: Coccolithophorids on the continental slope of the Bay of Biscay – production, transport and contribution to mass fluxes. Deep Sea Research Part II Topical Studies In Oceanography, 46(10), 2147-2174. https://doi.org/10.1016/s0967-0645(99)00058-2, 1999.

Beaufort, L., and Heussner, S.: Seasonal dynamics of calcareous nannoplankton on a West European continental margin: the Bay of Biscay. Marine Micropaleontology, 43(1-2), 27-55. https://doi.org/10.1016/s0377-8398(01)00020-2, 2001.

Beuvier, T., Probert, I., Beaufort, L., Suchéras-Marx, B., Chushkin, Y., Zontone, F., Gibaud, A.: X-ray nanotomography of coccolithophores reveals that coccolith mass and segment number correlate with grid size. Nature Communications, 10(1), 751. https://doi.org/10.1038/s41467-019-08635-x, 2019.

Boeckel, B. and Baumann, K.-H.: Vertical and lateral variations in coccolithophore community structure across the subtropical frontal zone in the South Atlantic Ocean. Marine Micropaleontology, 67, 255–273. https://doi.org/10.1016/j.marmicro.2008.01.014, 2008.

https://doi.org/10.5194/egusphere-2026-3055
Preprint. Discussion started: 26 June 2026

Bianco, S., Bordiga, M., Langer, G., Ziveri, P., Cerino, F., Di Giulio, A., and Lupi, C.: Low sensitivity of a heavily calcified coccolithophore under increasing CO2: the case study of Helicosphaera carteri. Biogeosciences, 22(7), 1821-1837. https://doi.org/10.5194/bg-22-1821-2025, 2025.

Bianco, S., Bordiga, M., Langer, G., Ziveri, P., Cerino, F., Relitti, F., Laudicella, V. A., Di Giulio, A., and Lupi, C.: Helicosphaera carteri (Prymnesiophyceae) under high carbon dioxide: An experimental study. Journal Of Phycology, 61(6), 1576-1590. https://doi.org/10.1111/jpy.70103, 2025.

Broecker, W. S. and Peng, T.-H.: Tracers in the Sea, Lamont-Doherty Geological Observatory, Columbia University Palisades, New York. https://science.whoi.edu/users/mcgillic/cruises/TN376/cruiseshare/Morton%20lab/Texts/Tracers%20in%20the%20Sea%20-%20Broecker%20_%20Peng.pdf (last access: 21 May 2026), 1982.

Brown, C. W. and Yoder, J. A.: Coccolithophorid blooms in the global ocean. Journal Of Geophysical Research Atmospheres, 99(C4), 7467-7482. https://doi.org/10.1029/93jc02156, 1994.

Buitenhuis, E. T., Quéré, C. L., Bednaršek, N., and Schiebel, R.: Large Contribution of Pteropods to Shallow $CaCO_3$ Export. Global Biogeochemical Cycles, 33(3), 458-468. https://doi.org/10.1029/2018gb006110, 2019.

Claustre, H., Sciandra, A., and Vaulot, D.: Introduction to the special section bio-optical and biogeochemical conditions in the South-East Pacific in late 2004: the BIOSOPE program. Biogeosciences, 5(3), 679-691. https://doi.org/10.5194/bg-5-679-2008, 2008.

Claustre, H. and Maritorena, S.: The many shades of ocean blue. Science, 302(5650), 1514–1515. https://doi.org/10.1126/science.1092704, 2003.

Cornec, M., Claustre, H., Mignot, A., Guidi, L., Lacour, L., Poteau, A., D'Ortenzio, F., Gentili, B., and Schmechtig, C.: Deep Chlorophyll Maxima in the Global Ocean: Occurrences, Drivers and Characteristics. Global Biogeochemical Cycles, 35(4), e2020GB006759. https://doi.org/10.1029/2020gb006759, 2021.

Cubillos, J. C., Henderiks, J., Beaufort, L., Howard, W. R., and Hallegraeff, G. M.: Reconstructing calcification in ancient coccolithophores: Individual coccolith weight and morphology of Coccolithus pelagicus (sensu lato). Marine Micropaleontology, 92, 29-39. https://doi.org/10.1016/j.marmicro.2012.04.005, 2012.

Daniels, C. J., Poulton, A. J., Balch, W. M., Marañón, E., Adey, T., Bowler, B. C., Cermeño, P., Charalampopoulou, A., Crawford, D. W., Drapeau, D., Feng, Y., Fernández, A., Fernández, E., Fragoso, G. M., González, N., Graziano, L. M., Heslop, R., Holligan, P. M., Hopkins, J., Huete-Ortega, M., Hutchins, D. A., Lam, P. J., Lipsen, M.S., López-Sandoval, D. C., Loucaides, S., Marchetti, A., Mayers, K. M. J., Rees, A. P., Sobrino, C., Tynan, E., and Tyrrell, T.: A global compilation of coccolithophore calcification rates. Earth System Science Data, 10(4), 1859-1876. https://doi.org/10.5194/essd-10-1859-2018, 2018.

Daniels, C., Poulton, A., Young, J., Esposito, M., Humphreys, M., Ribas-Ribas, M., Tynan, E., and Tyrrell, T.: Species-specific calcite production reveals Coccolithus pelagicus as the key calcifier in the Arctic Ocean. Marine Ecology Progress Series, 555, 29-47. https://doi.org/10.3354/meps11820, 2016.

Daniels, C.J., Sheward, R.M., Poulton, A.J.: Biogeochemical implications of comparative growth rates of Emiliania huxleyi and Coccolithus species. Biogeosciences 11(23), 6915-6925. https://doi.org/10.5194/bg-11-6915-2014, 2014.

De Bodt, C., Van Oostende, N., Harlay, J., Sabbe, K., and Chou, L.: Individual and interacting effects of pCO2 and temperature on Emiliania huxleyi calcification: study of the calcite production, the coccolith morphology and the coccosphere size. Biogeosciences, 7(5), 1401-1412. https://doi.org/10.5194/bg-7-1401-2010, 2010.

https://doi.org/10.5194/egusphere-2026-3055
Preprint. Discussion started: 26 June 2026

Dimiza, M. D., Triantaphyllou, M. V., Malinverno, E., Psarra, S., Karatsolis, B., Mara, P., Lagaria, A., and Gogou, A.: The composition and distribution of living coccolithophores in the Aegean Sea (NE Mediterranean). Micropaleontology, 61(6), 521-540. https://doi.org/10.47894/mpal.61.6.09, 2016.

Diner, R. E., Benner, I., Passow, U., Komada, T., Carpenter, E. J., and Stillman, J. H.: Negative effects of ocean acidification on calcification vary within the coccolithophore genus Calcidiscus. Marine Biology, 162(6), 1287-1305. https://doi.org/10.1007/s00227-015-2669-x, 2015.

Ellouz-Zimmermann, N., and Beaufort, L.: CARACALHIS/HAÏTI-BGF cruise, R/V L'Atalante. https://doi.org/10.17600/15006900, 2015.

Fiorini, S., Middelburg, J., and Gattuso, J.: Effects of elevated CO2 partial pressure and temperature on the coccolithophore Syracosphaera pulchra. Aquatic Microbial Ecology, 64(3), 221-232. https://doi.org/10.3354/ame01520, 2011.

Fuertes, M., Flores, J., and Sierro, F. J.: The use of circularly polarized light for biometry, identification and estimation of mass of coccoliths. Marine Micropaleontology, 113, 44-55. https://doi.org/10.1016/j.marmicro.2014.08.007, 2014.

Giraudeau, J.: Distribution of Recent nannofossils beneath the Benguela system: Southwest African continental margin. Marine Geology, 108(2), 219-237. https://doi.org/10.1016/0025-3227(92)90174-g, 1992.

Guerreiro, C. V., Ferreira, A., Cros, L., Stuut, J., Baker, A., Tracana, A., Pinto, C., Veloso, V., Rees, A. P., Cachão, M. A. P., Nunes, T., and Brotas, V.: Response of coccolithophore communities to oceanographic and atmospheric processes across the North- and Equatorial Atlantic. Frontiers In Marine Science, 10. https://doi.org/10.3389/fmars.2023.1119488, 2023.

Hagino, K., Okada, H., and Matsuoka, H.: Spatial dynamics of coccolithophore assemblages in the Equatorial Western-Central Pacific Ocean. Marine Micropaleontology, 39(1-4), 53-72. https://doi.org/10.1016/s0377-8398(00)00014-1, 2000.

Han, Y., Steiner, Z., Cao, Z., Fan, D., Chen, J., Yu, J., and Dai, M.: Coccolithophore abundance and production and their impacts on particulate inorganic carbon cycling in the western North Pacific. Biogeosciences, 22(14), 3681-3697. https://doi.org/10.5194/bg-22-3681-2025, 2025.

Hernández-Almeida, I., Ausín, B., Saavedra-Pellitero, M., Baumann, K., and Stoll, H.: Quantitative reconstruction of primary productivity in low latitudes during the last glacial maximum and the mid-to-late Holocene from a global Florisphaera profunda calibration dataset. Quaternary Science Reviews, 205, 166-181. https://doi.org/10.1016/j.quascirev.2018.12.016, 2018.

Jocher, G., Qiu, J., and Chaurasia, A.: Ultralytics YOLO (Version 8.0.0) [Computer software]. https://github.com/ultralytics/ultralytics, 2023.

Keuter, S., Silverman, J., Krom, M. D., Sisma-Ventura, G., Yu, J., Tsemel, A., Ben-Ezra, T., Sher, D., Reich, T., Koplovitz, G., and Frada, M. J.: Seasonal patterns of coccolithophores in the ultra-oligotrophic South-East Levantine Basin, Eastern Mediterranean Sea. Marine Micropaleontology, 175, 102153. https://doi.org/10.1016/j.marmicro.2022.102153, 2022.

Kinkel, H., Baumann, K., and ČEpek, M.: Coccolithophores in the equatorial Atlantic Ocean: response to seasonal and Late Quaternary surface water variability. Marine Micropaleontology, 39(1-4), 87-112. https://doi.org/10.1016/s0377-8398(00)00016-5, 2000.

https://doi.org/10.5194/egusphere-2026-3055
Preprint. Discussion started: 26 June 2026

Knecht, N. S., Benedetti, F., Elizondo, U. H., Bednaršek, N., Chaabane, S., De Weerd, C., Peijnenburg, K. T. C. A., Schiebel, R., and Vogt, M.: The Impact of Zooplankton Calcifiers on the Marine Carbon Cycle. Global Biogeochemical Cycles, 37(6). https://doi.org/10.1029/2022gb007685, 2023.

Kruijt, A. L., van Dijk, R., Sulpis, O., Beaufort, L., Lassus, G., Brummer, G.-J., van der Burg, A. D., Cala, B. A., Ourradi, Y., Peijnenburg, K. T. C. A., Humphreys, M. P., Chaabane, S., Sluijs, A., and Middelburg, J. J.: The contributions of various calcifying plankton to the South Atlantic calcium carbonate stock. Biogeosciences, 23, 531–563. https://doi.org/10.5194/bg-23-531-2026, 2026.

Krumhardt, K. M., Lovenduski, N. S., Iglesias-Rodriguez, M. D., and Kleypas, J. A.: Coccolithophore growth and calcification in a changing ocean. Progress In Oceanography, 159, 276-295. https://doi.org/10.1016/j.pocean.2017.10.007, 2017.

Langer, G., Nehrke, G., Probert, I., Ly, J., and Ziveri, P.: Strain-specific responses of Emiliania huxleyi to changing seawater carbonate chemistry. Biogeosciences, 6(11), 2637-2646. https://doi.org/10.5194/bg-6-2637-2009, 2009.

Longhurst, A. R.: Ecological geography of the sea, Academic Press, San Diego, 398 pp., 1998.

Millero, F. J.: The Marine Inorganic Carbon cycle. Chemical Reviews, 107(2), 308-341. https://doi.org/10.1021/cr0503557, 2007.

Milliman, J. D.: Production and accumulation of calcium carbonate in the ocean: Budget of a nonsteady state. Global Biogeochemical Cycles, 7(4), 927-957. https://doi.org/10.1029/93gb02524, 1993.

Neukermans, G., Bach, L., Butterley, A., Sun, Q., Claustre, H., and Fournier, G.: Quantitative and mechanistic understanding of the open ocean carbonate pump - perspectives for remote sensing and autonomous in situ observation. Earth-Science Reviews, 239, 104359. https://doi.org/10.1016/j.earscirev.2023.104359, 2023.

O'Brien, C. J., Peloquin, J. A., Vogt, M., Heinle, M., Gruber, N., Ajani, P., Andruleit, H., Arístegui, J., Beaufort, L., Estrada, M., Karentz, D., Kopczyńska, E., Lee, R., Poulton, A. J., Pritchard, T., and Widdicombe, C.: Global marine plankton functional type biomass distributions: coccolithophores. Earth System Science Data, 5(2), 259-276. https://doi.org/10.5194/essd-5-259-2013, 2013.

Okada, H., and Honjo, S.: The distribution of oceanic coccolithophorids in the Pacific. Deep Sea Research and Oceanographic Abstracts, 20(4), 355–374. https://doi.org/10.1016/0011-7471(73)90059-4, 1973.

Okada, H., and Honjo, S.: Distribution of coccolithophores in marginal seas along the western Pacific Ocean and in the Red Sea. Marine Biology, 31(3), 271-285. https://doi.org/10.1007/bf00387154, 1975.

Okada, H. and McIntyre, A.: Seasonal distribution of modern coccolithophores in the western North Atlantic Ocean. Marine Biology, 54(4), 319-328. https://doi.org/10.1007/bf00395438, 1979.

Poulton, A. J., Adey, T. R., Balch, W. M., and Holligan, P. M.: Relating coccolithophore calcification rates to phytoplankton community dynamics: Regional differences and implications for carbon export. Deep Sea Research Part II Topical Studies In Oceanography, 54(5-7), 538-557. https://doi.org/10.1016/j.dsr2.2006.12.003, 2007.

Poulton, A. J., Holligan, P. M., Charalampopoulou, A., and Adey, T. R.: Coccolithophore ecology in the tropical and subtropical Atlantic Ocean: New perspectives from the Atlantic meridional transect (AMT) program. Progress In Oceanography, 158, 150-170. https://doi.org/10.1016/j.pocean.2017.01.003, 2017.

Ras, J., Claustre, H., and Uitz, J.: Spatial variability of phytoplankton pigment distributions in the Subtropical South Pacific Ocean: comparison between in situ and predicted data. Biogeosciences, 5(2), 353-369. https://doi.org/10.5194/bg-5-353-2008, 2008.

https://doi.org/10.5194/egusphere-2026-3055
Preprint. Discussion started: 26 June 2026

Redmon, J., Divvala, S., Girshick, R., and Farhadi, A.: You Only Look Once: Unified, Real-Time Object Detection. In 2016 IEEE Conference on Computer Vision and Pattern Recognition (CVPR) (pp. 779–788). https://doi.org/10.1109/CVPR.2016.91, 2016.

Sarmiento, J. L., and Gruber, N.: Ocean Biogeochemical Dynamics. In Princeton University Press eBooks. https://doi.org/10.2307/j.ctt3fgxqx, 2013.

Schlitzer, R.: Ocean Data View, https://odv.awi.de, last access: 24 May 2026.

Sett, S., Bach, L. T., Schulz, K. G., Koch-Klavsen, S., Lebrato, M., and Riebesell, U.: Temperature Modulates Coccolithophorid Sensitivity of Growth, Photosynthesis and Calcification to Increasing Seawater pCO2. PLoS ONE, 9(2), e88308. https://doi.org/10.1371/journal.pone.0088308, 2014.

Shen, L., Ren, F., Wang, Y., Li, Z., Zheng, M., Li, X., Fan, W., Yang, Y., Sang, M., Liu, C., Han, G., Qin, S., Fan, J., Tian, L., Kuang, T., Shen, J., and Wang, W.: Structure and function of a huge photosystem I–fucoxanthin chlorophyll supercomplex from a coccolithophore. Science, 389(6765), eadv2132. https://doi.org/10.1126/science.adv2132, 2025.

Sulpis, O., Agrawal, P., Wolthers, M., Munhoven, G., Walker, M., and Middelburg, J. J.: Aragonite dissolution protects calcite at the seafloor. Nature Communications, 13(1), 1104. https://doi.org/10.1038/s41467-022-28711-z, 2022.

Sulpis, O., Jeansson, E., Dinauer, A., Lauvset, S. K., and Middelburg, J. J.: Calcium carbonate dissolution patterns in the ocean. Nature Geoscience, 14(6), 423-428. https://doi.org/10.1038/s41561-021-00743-y, 2021.

Suchéras-Marx, B., Viseur, S., Walker, C. E., Beaufort, L., Probert, I., and Bolton, C.: Coccolith size rules – What controls the size of coccoliths during coccolithogenesis. Marine Micropaleontology, 170, 102080. https://doi.org/10.1016/j.marmicro.2021.102080, 2021.

Sundquist, E. T., and Broecker, W. S.: The Carbon Cycle and Atmospheric CO2: Natural Variations, Archean to Present. Edited by: Sundquist, E. T. and Broecker, W. S., American Geophysical Union, Washington, D. C. https://doi.org/10.1029/GM032, 1985.

Šupraha, L., Gerecht, A. C., Probert, I., and Henderiks, J.: Eco-physiological adaptation shapes the response of calcifying algae to nutrient limitation. Scientific Reports, 5(1), 16499. https://doi.org/10.1038/srep16499, 2015.

Tyrrell, T., and Merico, A.: Emiliania huxleyi: bloom observations and the conditions that induce them. In Coccolithophores: from molecular processes to global impact. Berlin, Heidelberg: Springer Berlin Heidelberg (pp. 75-97). https://doi.org/10.1007/978-3-662-06278-4_4, 2004.

Valença, C. R., Beaufort, L., Hallegraeff, G. M., and Müller, M. N.: Technical note: A comparison of methods for estimating coccolith mass. Biogeosciences, 21(6), 1601-1611. https://doi.org/10.5194/bg-21-1601-2024, 2024.

Winter, A. M. O. S., and Siesser, W. G.: Atlas of living coccolithophores. Coccolithophores, 107-159, 1994.

Yang, M., Batchelor-McAuley, C., Barton, S., Rickaby, R. E. M., Bouman, H. A., and Compton, R. G.: Single-entity coccolithophore electrochemistry shows size is no guide to the degree of calcification. Environmental Science Advances, 1(2), 156-163. https://doi.org/10.1039/d2va00025c, 2022.

Young, J.R., Bown P.R., Lees J.A.: Nannotax3 website. International Nannoplankton Association. https://www.mikrotax.org/Nannotax3/ (last access: 24 August 2025), 2022.

Young, J. R., Geisen, M., Cros, L., Kleijne, A., Probert, I., and Ostergaard, J. B.: A guide to extant coccolithophore taxonomy. Journal Of Nannoplankton Research, S1, 1-132. https://doi.org/10.58998/jnr2297, 2003.

https://doi.org/10.5194/egusphere-2026-3055
Preprint. Discussion started: 26 June 2026

Young, J.R., and Ziveri, P.: Calculation of coccolith volume and its use in calibration of carbonate flux estimates. Deep-Sea Research Part II: Topical Studies in Oceanography 47, 1679-1700. https://doi.org/10.1016/S0967-0645(00)00003-5, 2000.

Ziveri, P., De Bernardi, B., Baumann, K., Stoll, H. M., and Mortyn, P. G.: Sinking of coccolith carbonate and potential contribution to organic carbon ballasting in the deep ocean. Deep Sea Research Part II: Topical Studies In Oceanography, 54(5-7), 659-675. https://doi.org/10.1016/j.dsr2.2007.01.006, 2007.

Ziveri, P., Gray, W. R., Anglada-Ortiz, G., Manno, C., Grelaud, M., Incarbona, A., Rae, J. W. B., Subhas, A. V., Pallacks, S., White, A., Adkins, J. F., and Berelson, W.: Pelagic calcium carbonate production and shallow dissolution in the North Pacific Ocean. Nature Communications, 14(1), 805. https://doi.org/10.1038/s41467-023-36177-w, 2023.

Ziveri, P., Langer, G., Chaabane, S., de Vries, J., Gray, W. R., Keul, N., Hatton, I. A., Manno, C., Norris, R., Pallacks, S., Young, J. R., Schiebel, R., Zarkogiannis, S., Anglada-Ortiz, G., Bianco, S., de Garidel-Thoron, T., Grelaud, M., Lucas, A., Probert, I., and Mortyn, P. G.: Calcifying plankton: From biomineralization to global change. Science, 390 (6771). https://www.science.org/doi/10.1126/science.adq8520, 2025.